UC San Diego

UC San Diego Electronic Theses and Dissertations

Title

Identifying neural mechanisms of sensorimotor feedback in action sequencing

Permalink

https://escholarship.org/uc/item/1jj608q8

Author

Huang, Hsiang-Hsuan

Publication Date

2022

Peer reviewed|Thesis/dissertation

eScholarship.org Powered by the California Digital Library
University of California

UNIVERSITY OF CALIFORNIA SAN DIEGO

Identifying neural mechanisms of sensorimotor feedback in action sequencing

A Dissertation submitted in partial satisfaction of the requirements
for the degree Doctor of Philosophy

in

Neurosciences

by

Hsiang-Hsuan Huang

Committee in charge:

Professor Xin Jin, Co-Chair
Professor Nicholas C. Spitzer, Co-Chair
Professor Edward M. Callaway
Professor Timothy Q. Gentner
Professor Christina M. Gremel

2022

Copyright

Hsiang-Hsuan Huang, 2022

All rights reserved.

The Dissertation of Hsiang-Hsuan Huang is approved, and it is acceptable in quality and form for publication on microfilm and electronically.

University of California San Diego

2022

DEDICATION

For my family and David

TABLE OF CONTENTS

LIST OF FIGURES

LIST OF ABBREVIATIONS

AAV	adeno-associated virus
ACC	anterior cingulate cortex
AuD	auditory cortex
Cg	cingulate cortex
ChR2	channelrhodopsin 2
DA	dopamine
DLS	dorsolateral striatum
DMS	dorsomedial striatum
dSPNs	direct pathway striatal projection neurons
GFP	green fluorescent protein
iSPNs	indirect pathway striatal projection neurons
M1	primary motor cortex
M2	secondary motor cortex
PL	prelimbic cortex
PPC	posterior parietal cortex
OFC	orbitofrontal cortex
SCZ	schizophrenia
SMA	supplementary motor areas
vGAT	vesicular glutamate transporter

ACKNOWLEDGEMENTS

I would like to acknowledge my advisor Xin Jin for your insight, scientific guidance, and mentorship over the past six years. Thank you for motivating me and guiding me along this journey. I would also like to thank my doctoral committee members – Drs. Nick Spitzer, Ed Callaway, Tina Gremel, Tim Gentner, and Chris Kintner for your support and critical scientific advice over the past years. I would like to thank my colleague Sho Aoki for your mentorship and scientific inputs. I would like to acknowledge Xunyi Yan for slice recording and all kinds of support throughout this long journey. I would like to acknowledge Baibing Zhang for sharing the slice recording data and training *in vivo* recording. I would like to thank Hao Li for training when I first joined the lab and for advice on *in vivo* recording. I would like to thank Xiaochun Cai for being an inspiring lab mate and for all your support. I also really appreciate each former member of Jin lab for playing an important role in my growth along the way.

I would like to thank the fantastic people in the UCSD neurosciences graduate program for being inspiring and supportive. I am also grateful for the financial support from the Salk Women & Science Special Award.

Finally, I would like to thank my parents and David Kuo for your all-time support.

Chapter 1-5, in part, is currently being prepared for submission for publication of the material. Huang, Hsiang-Hsuan; Yan, Xunyi; Zhang, Baibing; Jin, Xin. The dissertation author was the primary researcher and author of this material.

VITA

2009 Doctor of Medicine, National Taiwan University

2022 Doctor of Philosophy in Neurosciences, University of California San Diego

PUBLICATIONS

Cook, J. R., Li, H., Nguyen, B., **Huang, H. H.**, Mahdavian, P., Kirchgessner, M. A., . . . Jin, X. (2022). Secondary auditory cortex mediates a sensorimotor mechanism for action timing. *Nat Neurosci, 25*(3), 330-344. doi:10.1038/s41593-022-01025-5

Li, C. T., Hsieh, J. C., **Huang, H. H.**, Chen, M. H., Juan, C. H., Tu, P. C., . . . Su, T. P. (2016). Cognition-Modulated Frontal Activity in Prediction and Augmentation of Antidepressant Efficacy: A Randomized Controlled Pilot Study. *Cereb Cortex, 26*(1), 202-210. doi:10.1093/cercor/bhu191

Li, C. T., Chen, M. H., Juan, C. H., **Huang, H. H.**, Chen, L. F., Hsieh, J. C., . . . Su, T. P. (2014). Efficacy of prefrontal theta-burst stimulation in refractory depression: a randomized sham-controlled study. *Brain, 137*(Pt 7), 2088-2098. doi:10.1093/brain/awu109

Huang, H.H., Hong, C.J., Yeh, H.L., Liou, Y.J., Yang, A.C., Liu, M.E., Tsai, S.J. (2012). "Dopamine D2 receptor gene Taq1 A polymorphism is associated with cognitive performance in elderly males without dementia." Taiwanese Journal of Psychiatry, 26(1):32-40.

Huang, H. H., Wang, Y. C., Wu, C. L., Hong, C. J., Bai, Y. M., Tsai, S. J., & Liou, Y. J. (2011). TNF-alpha -308 G>A polymorphism and weight gain in patients with schizophrenia under long-term clozapine, risperidone or olanzapine treatment. *Neurosci Lett, 504*(3), 277-280. doi:10.1016/j.neulet.2011.09.046

Huang, H. H., & Bai, Y. M. (2011). Persistent psychosis after ingestion of a single tablet of '2C-B'. *Prog Neuropsychopharmacol Biol Psychiatry, 35*(1), 293-294. doi:10.1016/j.pnpbp.2010.10.018

ABSTRACT OF THE DISSERTATION

Identifying neural mechanisms of sensorimotor feedback in action sequencing

by

Hsiang-Hsuan Huang

Doctor of Philosophy in Neurosciences

University of California San Diego, 2022

Professor Xin Jin, Co-Chair
Professor Nicholas C. Spitzer, Co-Chair

Our everyday behavior is composed of diversified action sequences. Rapid integration of real-time sensory feedback with action enables rather swift, effortless execution of the learned sequences. Sensorimotor integration is the process through which the brain matches motor commands to the sensory consequence arising from their execution. It has been proposed that our brain uses an internal forward model to predict sensory outcomes of motor commands. The compatibility between actual and predicted sensory feedback indicates successful execution of an action and is crucial for the sense of self-ownership of action. Disruption in sensorimotor integration not only sabotages action sequencing but also compromises self-agency and is implicated in agency-related psychotic symptoms. Where and how sensorimotor integration occurs in mammalian brains, however, remains elusive. Songbirds have been the most prominent model in studying the role of auditory feedback in motor sequencing, and mouse models are relatively few in this field. In this dissertation, I describe my efforts in establishing a mouse model to explore auditory-motor integration in action sequencing. I designed a behavior task in which mice learn to perform a heterogeneous action sequence with the assistance of artificial auditory feedback. Using a comprehensive approach with viral tracing, optogenetics, chemogenetics, and both in vivo and slice electrophysiological recordings, I demonstrate the role of the cingulate cortex and the medial portion of the secondary motor cortex in integrating sensorimotor feedback and controlling the switch between subsequences– a crucial decision for successful performance. I also identified two parallel corticostriatal pathways that coordinately regulate sensory feedback-based action sequencing. Our findings reveal an essential neural mechanism of sensorimotor feedback in action sequencing. In the final part of the dissertation, by reviewing current literature I also discuss how the findings of the present study could provide critical insights and a comprehensive perspective in understanding the pathophysiology of schizophrenia.

Chapter 1: Introduction and Background

1.1 Action sequencing

1.1.1 Action sequencing is the foundation of behavior

Action sequences form the foundation of human and animal behavior. Whether to speak, play an instrument, or generate trains of thought, the subject needs to perform a series of motor or cognitive movements in precise timing and order. That being said, the brain does not simply execute the whole series of movements mechanically; instead, the brain is thought to organize individual elements into functional units of action sequences (Lashley, 1951; Gallistel, 1981; Graybiel, 1998). The advantage of chunking relevant pieces of information into separate units is that the brain can perform efficiently despite the limited capacity of storage (Miller, 1956; Jin & Costa, 2015). Several studies support this idea by showing that humans and other species demonstrate the pattern of 'chunking' during behavior, and by doing so behavioral efficiency is increased (Sakai, Kitaguchi, & Hikosaka, 2003; Wymbs, Bassett, Mucha, Porter, & Grafton, 2012; reviewed in Jin & Costa, 2015). It is further supported by the observation that neuronal activity corresponding to the initiation or termination of each action sequence emerges following learning (Jin & Costa, 2010). It was proposed that the system which generates movements is hierarchically organized, from the basic elementary action units to higher coordinating units and then the highest command units (Gallistel, 1981). Although the hierarchical view of action sequence control is well accepted through rigorous behavioral analyses, as opposed to the response chains theory, it was until

recently that this framework was experimentally confirmed with compelling evidence (Geddes et al., 2018).

1.1.2 Basal ganglia

The basal ganglia comprise a group of interconnected subcortical nuclei– the striatum, the substantia nigra (the pars compacta (SNc) and the pars reticulata (SNr)), the globus pallidus (the internal segment (GPi), and the external segment (GPe)), and the subthalamic nucleus (STN) – and are critical for motor and cognitive functions (Gerfen & Surmeier, 2011; Kreitzer & Malenka, 2008; Shepherd, 2013). The dysfunction of basal ganglia circuits is implicated in a wide range of neurological and psychiatric diseases, such as Parkinson's disease, Huntington's disease (Albin, Young, & Penney, 1989; DeLong, 1990), obsessive-compulsive disorder (Graybiel & Rauch, 2000), and schizophrenia (McCutcheon, Abi-Dargham, & Howes, 2019). The striatum is the primary input nucleus of basal ganglia and receives multimodal information all over from the cortex and computes to achieve action selection. Information from the striatum is conveyed to the rest of basal ganglia through GABAergic striatal projection neurons (SPNs) of the direct and indirect pathways. Dopamine D1 receptor-expressing SPNs (dSPNs) in the direct pathway project monosynaptically to SNr and GPi; dopamine D2 receptor-expressing SPNs (iSPNs) project polysynaptically to SNr via first GPe and secondly STN. The main output nucleus SNr then transmits information to the thalamus, which projects to back the cortex to form functional cortico-striatal-thalamo-cortical (CSTC) loops (Gerfen & Surmeier, 2011). Three major parallel complementary CSTC pathways have been identified to process sensorimotor, limbic, and associative

information, respectively. (Jahanshahi, Obeso, Rothwell, & Obeso, 2015). Classic models of basal ganglia proposed a competition between the direct and indirect pathways in action selection and modulation: the former facilitates actions, and the latter inhibits actions. (Albin et al., 1989; Alexander & Crutcher, 1990; DeLong, 1990). Accumulating evidence from recent studies, however, suggests that these two pathways work coordinately to achieve action control (Cui et al., 2013; Isomura et al., 2013; Jin, Tecuapetla, & Costa, 2014; Tecuapetla, Jin, Lima, & Costa, 2016; Geddes et al., 2018).

1.1.3 Action sequencing and basal ganglia circuits

A rich body of evidence suggests that the striatum is critical for the shaping and execution of action sequences (Doupe, Perkel, Reiner, & Stern, 2005; Graybiel, 1998; Hikosaka et al., 1999; Jin & Costa, 2010, 2015; Jin et al., 2014; Wymbs et al., 2012; Geddes et al., 2018). Patients with diseases associated with basal ganglia dysfunction demonstrate clear impairment in action sequence organization (Benecke, Rothwell, Dick, Day, & Marsden, 1987; Boyd et al., 2009). Synaptic plasticity in the dorsal striatum is crucial for action sequence learning. Selective deletion of NMDA receptors in striatal projection neurons (SPNs) impairs corticostriatal plasticity and animals' ability to acquire and consolidate action sequences (Jin & Costa, 2010; Geddes et al., 2018). Recordings of neuronal activity in the dorsal striatum revealed that a large proportion of SPNs show phasic changes in activity associated with the initiation or termination of a sequence consisting of a single type of action. This start/stop activity increasingly emerges after learning (Jin & Costa, 2010, 2015).

With further identification of cell types, it was found that the direct and indirect pathways are concurrently activated around sequence start/stop, and have different activity patterns during sequence performance– more dSPNs show sustained activity, while more iSPNs show inhibited activity. At the sequence initiation, the activated dSPNs could serve to select the desired program, and the activated iSPNs could shut down the competing programs. During the execution of the sequence, sustained activity from dSPNs could facilitate the selected action (Jin et al., 2014; Jin & Costa, 2015). These results demonstrate that the control of action sequence required cooperation, rather than mere competition, between the direct and indirect pathways.

To interrogate whether the action sequence is hierarchically organized and how it is controlled by the direct and indirect pathways, Geddes (2018) trained mice to perform a heterogeneous action sequence. In this self-paced task, the animals learn to press the separate left and right levers in the ‘‘left-left-right-right’’ order. This “LLRR” action sequence features a specific spatiotemporal pattern and is composed of two subsequences LL and RR. As a result, performing this action sequence requires a “switch” phase between subsequences, in addition to the start and stop. With optogenetic manipulation of dSPNs and iSPNs, their results highly suggest a hierarchical organization underlying action sequences. Moreover, dSPNs and iSPNs behave differently at each level of the sequence hierarchy and coordinate during sequence execution. At the sequence level, both dSPNs and iSPNs are active to signal start/stop. At the subsequence level, iSPNs control the switch between subsequences. At the element level, more dSPNs display sustained activity, while more iSPNs display inhibited activity. Overall, the coordinating roles of the direct and indirect pathways are consistent with

those in action sequences composed of the same elements (Jin et al., 2014) and they further demonstrate that the indirect pathway predominantly controls the switch between-subsequence in heterogeneous action sequences. The activity of a large proportion of iSPNs increases exclusively during the behavioral switch. Optogenetically activation of iSPNs mediates switches whereas activation of dSPNs facilitates the ongoing action, indicating the complementary roles of these two pathways in execution of action sequences.

1.1.4 Future directions

Two further questions I attempted to answer in this dissertation are (1) how different cortical regions interact with the striatal pathways to control action sequencing and (2) the roles of sensory feedback play in action sequencing and the underlying neural mechanisms. The following chapters describe that I exploited multidisciplinary techniques to demonstrate two essential and parallel corticostriatal pathways controlling action sequencing in an artificial sensory feedback-assisted action sequence task.

1.2 Sensorimotor integration

1.2.1 Sensorimotor integration is fundamental to human and animal behavior

Self-consciousness is a feature considered unique to human beings– we are conscious of our agency, our own actions, and our thoughts. What is the 'self', then, is the most fundamental question that people often ask themselves. Self is a rather broad concept and could involve longitudinal personal identity and continuity– a narrative self. In contrast, a minimal self refers to a more primary and immediate experience: the sense of self-agency and self-ownership for actions (Gallagher, 2000). For example, what shapes the clear boundaries between self and the rest of the world? How is one sure that a thought or an action is coming from oneself? Human and animals perceive the world while influencing it; this perceptual experience is a dynamic process because their actions also constantly change the environment around them. Multisensory integration and more importantly, sensorimotor integration– the process through which the nervous system matches motor commands to the sensory consequence arising from their execution – are crucial for generating a sense of self-agency. The compatibility between an action and its sensory outcomes serves as strong evidence for the ownership of the action. (Gallagher, 2000; Jeannerod, 2003; Tsakiris, Schutz-Bosbach, & Gallagher, 2007). The ability to distinguish self-generated sensory signals, or sensory feedback, from environmental sensory signals is also essential to survival in the constantly changing world. For example, self-generated sounds of an animal are generally perceived as harmless and ignorable, and should not elicit a false alarm indicating coming from potential predators. Decreased sensitivity to self-generated sounds would also allow animals more tuned to auditory signals for food sources and social needs, etc. Indeed, attenuation of cortical

responses to self-generated sounds is a well-recognized phenomenon in human, non-human primates, and rodents (Curio, Neuloh, Numminen, Jousmaki, & Hari, 2000; Eliades & Wang, 2008; Ford, Mathalon, Heinks, et al., 2001; Schneider, Sundararajan, & Mooney, 2018; Weiss, Herwig, & Schutz-Bosbach, 2011). Moreover, our everyday behavior comprises a diverse repertoire of action sequences in dynamic environments. Mechanisms which enable element-based integration of real-time sensory feedback with action, error monitoring, and rapid correction/updates of motor commands are necessary for individuals to perform action sequences swiftly and accurately appropriate to various contexts.

1.2.2 Internal models and the role of sensory feedback

The process of sensorimotor integration involves the comparison of actual sensory feedback with predicted sensory consequences of actions. In this regard, internal representations of expected sensory outcomes resulting from the execution of motor commands are critical. The idea that the brain uses an internal model simulating the body and environment to predict the consequences of our own actions is well-established in motor control theory (Wolpert, Ghahramani, & Jordan, 1995; Miall & Wolpert, 1996; Blakemore, Goodbody, & Wolpert, 1998). This model is called an internal forward model as it makes a forward prediction for the causality between actions and the sensory consequences. According to Wolpert (1995), there are several reasons that justify the necessity of a forward model in motor control: (1) Sensory feedback always comes with significant delays in most sensorimotor loops. A motor control system purely relying on sensory feedback is too slow for rapid movements. Instead, with a forward model, an estimate of sensory consequences can

be made and used before sensory feedback is available. (2) A forward model is needed in a system that expects and cancels the sensory effects resulting from one's own action. (3) A forward model computes errors between the desired and actual sensory outcome, transforms this information into errors in the motor commands, and provides instructive signals for learning. (4) A forward model can generate a state estimate as part of a model which combines the state estimate and sensory discrepancy to predict the next state.

It has been proposed that upon the transmission of a motor command, an efference copy–a copy of the motor command– is sent to the internal model to make a prediction of sensory outcome; this representation is called 'corollary discharge' (Wolpert, Ghahramani, & Jordan, 1995; Blakemore, Goodbody, & Wolpert, 1998). The predicted sensory feedback will be compared with the actual feedback which arrives later, and the mismatch between these two is computed as prediction errors. Prediction errors can further inform an internal inverse model, which inversely calculates the motor command needed between a current and desired state, to generate corrective signals to modify the motor command for the next movement in the action sequence (Subramanian, Alers, & Sommer, 2019; Wolpert et al., 1995). This process serves as an essential mechanism for performance monitoring, which is important for learning and maintenance of behavior. Sensorimotor learning is a process of reducing the deviation between desired and actual performance through trial-and-error and reinforcement learning (Murphy, James, Sakata, & Prather, 2017). Therefore, monitoring sensory feedback and the deviation from expected feedback on an element basis, and modifying action accordingly, are critical for action sequence acquisition. After an action sequence is learned, carefully monitoring sensory feedback during execution is as important

for detecting behavior errors and fine-tuning ongoing action to achieve sophisticated performance. On the other hand, recurrent prediction errors also update the internal forward model to make a new prediction about the sensory outcome of an action. This allows behavioral flexibility in a constantly changing environment.

A prominent example of how the failure of integrating sensory feedback with action sabotages learning and execution of action sequences is the importance of auditory feedback in human speech and musical performance. Auditory feedback is critical in speech learning in early childhood, and as equally important in maintaining normal speech throughout adult life. It is known that people with congenital hearing impairment struggle with speech production. Acquired hearing impairment after normal speech is formed also causes speech deterioration over time (Ryalls, 1994). Perturbation of the real-time auditory speech feedback to the speaker's ear is a frequently used method to study auditory-motor integration during speech. For example, delayed auditory feedback (DAF), imposing a short delay in the voice/sound to the ear, has been shown to largely disrupt speech and other forms of action sequencing, such as musical performance and tapping. Common behavioral changes include slow performance rate, high variability, and increased errors of insertion and repetition. (Finney & Warren, 2002; Black, 1951; Finney, 1997; Zimmermann, Brown, Kelso, Hurtig, & Forrest, 1988). Altered auditory feedback (AAF), another type of manipulation often involving omitted feedback or altered feedback pitch, also leads to disrupted action sequencing in both speech and musical performance. (Pfordresher & Beasley, 2014; Pruitt & Pfordresher, 2015) Another example to demonstrate the indispensability of sensory feedback in action sequencing is gait disturbance in patients with sensory ataxia. Sensory ataxia is caused by somatosensory

impairment, such as peripheral sensory neuropathy, which leads to disrupted transmission of somatosensory signals. The patients lose normal somatosensory feedback when their sole of the foot touches the ground. As a result, they suffer from discoordinated gaits even with intact motor systems, and often lift their legs to step heavily on the ground as compensation, known as trampling gait (Zhang, Zhou, Li, Yang, & Abbasi, 2021).

1.2.3 Sensorimotor integration, self-agency, and psychosis

The internal model for sensorimotor integration is not only useful for accounting for motor behavior but also has been expanded to understand cognitive processing. Indeed, thinking can be viewed as a complex form of mental action sequencing. As how Irwin Feinberg (2011) interprets Hughlings Jackson (1958)'s statement: "although the highest motor centers of thinking act without producing actual sensory reactions in the outside world, they would cause the sensory consequences on the sensory centers of consciousness that represent 'self' in most complex ways" (Feinberg 2011).

The idea of 'corollary discharge'–the representation of predicted sensory outcome for action– was first introduced in the 1920s. In studying how the brain distinguishes visual representation resulting from moving objects or from eye movements, Helmholtz (1925) first hypothesized the existence of a mechanism for forward prediction for action. This hypothesis was later supported experimentally by Von Holst and Mittelstaedt (1950) and Sperry (1950), suggesting that an efference copy of action generates a corollary discharge for motor prediction in the sensory cortex. In 1978, Irwin Feinberg first applied mechanisms of

sensorimotor integration to explain thinking, as a motor act at the highest level. He argued that thinking requires successful integration of corollary discharge and internal feedback in the brain and proposed that disrupted integration underlies psychotic symptoms in schizophrenia (Feinberg, 1978, 2011).

Auditory verbal hallucination is the most common symptom in patients with schizophrenia and is proposed to stem from aberrant integration during processing inner speech (Seal, Aleman, & McGuire, 2004; Jones & Fernyhough, 2007). When the motor command triggers inner speech, it will lead to auditory perceptual experience inside the brain; at the same time, an efferences copy will be used to generate corollary discharge encoding the predicted sensory outcome. The agreement between actual and predicted experience gives the subject a sense of ownership of the inner speech. In contrast, disrupted integration of corollary discharge impairs the ownership of the action, causing the subject to assign the voices of his or her own inner speech to someone else's. Other agency-related psychotic symptoms include thought insertion or delusion of being controlled are also believed to be attributed to similar dysfunctions. Moreover, the mismatch between actual and predicted sensory feedback will also impair the sense of self-agency and cause perceptual incoherence. These in turn contribute to a more pervasive and detrimental experience (yet often downplayed by the current diagnostic system)— the blurring of self-boundaries. Even after remission of prominent hallucination or delusions, some patients still report disturbed self-experiences, such as depersonalization, ambivalence, and a diminished sense of agency (Postmes et al., 2014). This experience was vividly described by Clara Kean (2009): "…the real 'me' is not here anymore. I am disconnected, disintegrated, diminished. Everything I experience is

through a dense fog, created by my own mind, yet it also resides outside my mind. I feel that my real self has left me, seeping through the fog toward a separate reality, which engulfs and dissolves this self. This has nothing to do with the suspicious thoughts or voices; it is purely a distorted state of being." Last but not least, formal thought disorder–disturbance in the organization of thinking– is also commonly seen in patients with schizophrenia. It is often characterized by poverty of content, incoherence, tangentiality, and loosening of association. It has been proposed that internal sensory feedback is essential for the hierarchical programming of thought processes. Disruption in integrating internal feedback therefore would lead to impaired mental action sequencing (Feinberg, 1978).

Although the framework proposed by Feinberg cannot be experimentally proved due to the nature of cognitive processes, accumulating evidence continues to lend support to it by showing that patients with schizophrenia display impaired corollary discharge signaling. It has been suggested that corollary discharge resulting from a self-generated action serves to suppress the neural responses in the sensory cortex. The sensory attenuation of self-generated movements explains why people cannot tickle themselves (Blakemore, Wolpert, & Frith, 1998). However, compelling studies showed that patients with schizophrenia have significantly smaller sensory attenuation of self-generated responses in multiple sensorimotor domains, such as tactile sensation and speech perception (Blakemore, Smith, Steel, Johnstone, & Frith, 2000; Ford, Mathalon, Heinks, et al., 2001; Ford, Mathalon, Kalba, et al., 2001; Shergill, Samson, Bays, Frith, & Wolpert, 2005). Studies on the oculomotor systems also strongly suggested disrupted corollary discharge in the patients (Thakkar & Rolfs, 2019). All together these results indicate sensorimotor integration deficits in schizophrenia.

1.2.4 Future directions

Despite the theoretical framework of sensorimotor integration using internal models being well-formulated, the neural substrates which integrate sensory feedback and representation of motor signals remain largely unknown. Studies have previously demonstrated a direct pathway from motor cortical inputs to the auditory cortex that serves as corollary discharge to suppress the auditory cortical responses to self-generated sound in mice (Schneider, Nelson, & Mooney, 2014; Schneider et al., 2018). However, it remains enigmatic where and how the sensory feedback and the motor representation are integrated to control action sequencing. In the present study, I designed an artificial auditory feedback-assisted action sequence task to investigate this question in mice. Although songbirds have been the most prominent model in studying the role of auditory feedback in motor sequencing, establishing mouse models to address this question is important in many ways. First, we can train free-moving mice to learn or relearn a variety of auditory-guided action sequences optimal for different experimental purposes. In contrast, birdsongs have fixed templates, lack spatial dimension, and relearning is not possible. In addition, the auditory cortex of songbirds does not display sensory attenuation to self-generated sounds, as observed in human, primates and rodents (Schneider & Mooney, 2018), indicating possible species differences in sensorimotor integration. It has been shown that in songbirds, sensory feedback signal is transmitted to the ventral tegmental area (VTA) which serves as a 'critic' and directly reinforces the basal ganglia (area X) to modulate song production (Kearney, Warren, Hisey, Qi, & Mooney, 2019), without a higher center integrating both sensory and motor information. In the following chapters, I described my efforts in elucidating where and how

sensory feedback is integrated in the mouse brain to assist action sequence execution. We identified a prefrontal cortical region that is critical in integrating sensorimotor feedback and utilizing the information to guide behavioral switching within the sequence via an associative corticostriatal circuit. We further demonstrate this associative corticostriatal pathway works with a sensorimotor corticostriatal pathway coordinatively in controlling action sequencing.

Part of chapter 1, in part, is currently being prepared for submission for publication of the material. (Huang, Hsiang-Hsuan; Yan, Xunyi; Zhang, Baibing; Jin, Xin.) The dissertation author was the primary researcher and author of this material.

References

Albin, R. L., Young, A. B., & Penney, J. B. (1989). The functional anatomy of basal ganglia disorders. *Trends Neurosci, 12*(10), 366-375. doi:10.1016/0166-2236(89)90074-x

Alexander, G. E., & Crutcher, M. D. (1990). Functional architecture of basal ganglia circuits: neural substrates of parallel processing. *Trends Neurosci, 13*(7), 266-271. doi:10.1016/0166-2236(90)90107-l

Benecke, R., Rothwell, J. C., Dick, J. P., Day, B. L., & Marsden, C. D. (1987). Disturbance of sequential movements in patients with Parkinson's disease. *Brain, 110 (Pt 2)*, 361-379. doi:10.1093/brain/110.2.361

Black, J. W. (1951). The Effect Of Delayed Side-Tone Upon Vocal Rate And Intensity. *Journal of Speech and Hearing Disorders, 16*(1), 56-60. doi:DOI 10.1044/jshd.1601.56

Blakemore, S. J., Goodbody, S. J., & Wolpert, D. M. (1998). Predicting the consequences of our own actions: The role of sensorimotor context estimation. *Journal of Neuroscience, 18*(18), 7511-7518. Retrieved from <Go to ISI>://WOS:000075893000042

Blakemore, S. J., Smith, J., Steel, R., Johnstone, C. E., & Frith, C. D. (2000). The perception of self-produced sensory stimuli in patients with auditory hallucinations and passivity experiences: evidence for a breakdown in self-monitoring. *Psychol Med, 30*(5), 1131-1139. doi:10.1017/s0033291799002676

Blakemore, S. J., Wolpert, D. M., & Frith, C. D. (1998). Central cancellation of self-produced tickle sensation. *Nat Neurosci, 1*(7), 635-640. doi:10.1038/2870

Boyd, L. A., Edwards, J. D., Siengsukon, C. S., Vidoni, E. D., Wessel, B. D., & Linsdell, M. A. (2009). Motor sequence chunking is impaired by basal ganglia stroke. *Neurobiol Learn Mem, 92*(1), 35-44. doi:10.1016/j.nlm.2009.02.009

Cui, G., Jun, S. B., Jin, X., Pham, M. D., Vogel, S. S., Lovinger, D. M., & Costa, R. M. (2013). Concurrent activation of striatal direct and indirect pathways during action initiation. *Nature, 494*(7436), 238-242. doi:10.1038/nature11846

Curio, G., Neuloh, G., Numminen, J., Jousmaki, V., & Hari, R. (2000). Speaking modifies voice-evoked activity in the human auditory cortex. *Hum Brain Mapp, 9*(4), 183-191. doi:10.1002/(sici)1097-0193(200004)9:4<183::aid-hbm1>3.0.co;2-z

DeLong, M. R. (1990). Primate models of movement disorders of basal ganglia origin. *Trends Neurosci, 13*(7), 281-285. doi:10.1016/0166-2236(90)90110-v

Doupe, A. J., Perkel, D. J., Reiner, A., & Stern, E. A. (2005). Birdbrains could teach basal ganglia research a new song. *Trends Neurosci, 28*(7), 353-363. doi:10.1016/j.tins.2005.05.005

Eliades, S. J., & Wang, X. (2008). Neural substrates of vocalization feedback monitoring in primate auditory cortex. *Nature, 453*(7198), 1102-1106. doi:10.1038/nature06910

Feinberg, I. (1978). Efference copy and corollary discharge: implications for thinking and its disorders. *Schizophr Bull, 4*(4), 636-640. doi:10.1093/schbul/4.4.636

Feinberg, I. (2011). Corollary discharge, hallucinations, and dreaming. *Schizophr Bull, 37*(1), 1-3. doi:10.1093/schbul/sbq115

Finney, S. A. (1997). Auditory feedback and musical keyboard performance. *Music Perception, 15*(2), 153-174. Retrieved from <Go to ISI>://WOS:000071268000004

Finney, S. A., & Warren, W. H. (2002). Delayed auditory feedback and rhythmic tapping: Evidence for a critical interval shift. *Perception & Psychophysics, 64*(6), 896-908. doi:Doi 10.3758/Bf03196794

Ford, J. M., Mathalon, D. H., Heinks, T., Kalba, S., Faustman, W. O., & Roth, W. T. (2001). Neurophysiological evidence of corollary discharge dysfunction in schizophrenia. *Am J Psychiatry, 158*(12), 2069-2071. doi:10.1176/appi.ajp.158.12.2069

Ford, J. M., Mathalon, D. H., Kalba, S., Whitfield, S., Faustman, W. O., & Roth, W. T. (2001). Cortical responsiveness during talking and listening in schizophrenia: an event-related brain potential study. *Biol Psychiatry, 50*(7), 540-549. doi:10.1016/s0006-3223(01)01166-0

Gallagher, I. I. (2000). Philosophical conceptions of the self: implications for cognitive science. *Trends Cogn Sci, 4*(1), 14-21. doi:10.1016/s1364-6613(99)01417-5

Gallistel, C.R. (1980). The organization of action: a new synthesis. Hillsdale (NJ): Lawrence Erlbaum Associates 13, 432

Geddes, C. E., Li, H., & Jin, X. (2018). Optogenetic Editing Reveals the Hierarchical Organization of Learned Action Sequences. *Cell, 174*(1), 32-43 e15. doi:10.1016/j.cell.2018.06.012

Gerfen, C. R., & Surmeier, D. J. (2011). Modulation of striatal projection systems by dopamine. *Annu Rev Neurosci, 34*, 441-466. doi:10.1146/annurev-neuro-061010-113641

Graybiel, A. M. (1998). The basal ganglia and chunking of action repertoires. *Neurobiol Learn Mem, 70*(1-2), 119-136. doi:10.1006/nlme.1998.3843

Graybiel, A. M., & Rauch, S. L. (2000). Toward a neurobiology of obsessive-compulsive disorder. *Neuron, 28*(2), 343-347. doi:10.1016/s0896-6273(00)00113-6

Hikosaka, O., Nakahara, H., Rand, M. K., Sakai, K., Lu, X., Nakamura, K., . . . Doya, K. (1999). Parallel neural networks for learning sequential procedures. *Trends Neurosci, 22*(10), 464-471. doi:10.1016/s0166-2236(99)01439-3

von Helmholtz H. In: Southall JPC ed. Physiological Optics. 3rd ed Menasha, WI: Banta; Vol. 3 (1925)243–246.

Isomura, Y., Takekawa, T., Harukuni, R., Handa, T., Aizawa, H., Takada, M., & Fukai, T. (2013). Reward-modulated motor information in identified striatum neurons. *J Neurosci, 33*(25), 10209-10220. doi:10.1523/JNEUROSCI.0381-13.2013

Jahanshahi, M., Obeso, I., Rothwell, J. C., & Obeso, J. A. (2015). A fronto-striato-subthalamic-pallidal network for goal-directed and habitual inhibition. *Nat Rev Neurosci, 16*(12), 719-732. doi:10.1038/nrn4038

Jeannerod, M. (2003). The mechanism of self-recognition in humans. *Behav Brain Res, 142*(1-2), 1-15. doi:10.1016/s0166-4328(02)00384-4

Jin, X., & Costa, R. M. (2010). Start/stop signals emerge in nigrostriatal circuits during sequence learning. *Nature, 466*(7305), 457-462. doi:10.1038/nature09263

Jin, X., & Costa, R. M. (2015). Shaping action sequences in basal ganglia circuits. *Curr Opin Neurobiol, 33*, 188-196. doi:10.1016/j.conb.2015.06.011

Jin, X., Tecuapetla, F., & Costa, R. M. (2014). Basal ganglia subcircuits distinctively encode the parsing and concatenation of action sequences. *Nat Neurosci, 17*(3), 423-430. doi:10.1038/nn.3632

Jones, S. R., & Fernyhough, C. (2007). Thought as action: inner speech, self-monitoring, and auditory verbal hallucinations. *Conscious Cogn, 16*(2), 391-399. doi:10.1016/j.concog.2005.12.003

Jordan, M. I., & Rumelhart, D. E. (1992). Forward Models - Supervised Learning with a Distal Teacher. *Cognitive Science, 16*(3), 307-354. doi:DOI 10.1207/s15516709cog1603_1

Kean, C. (2009). Silencing the Self: Schizophrenia as a Self-disturbance. *Schizophrenia Bulletin, 35*(6), 1034-1036. doi:10.1093/schbul/sbp043

Kearney, M. G., Warren, T. L., Hisey, E., Qi, J., & Mooney, R. (2019). Discrete Evaluative and Premotor Circuits Enable Vocal Learning in Songbirds. *Neuron, 104*(3), 559-575 e556. doi:10.1016/j.neuron.2019.07.025

Kreitzer, A. C., & Malenka, R. C. (2008). Striatal plasticity and basal ganglia circuit function. *Neuron, 60*(4), 543-554. doi:10.1016/j.neuron.2008.11.005

Lashley, K.S. (1951). The problem of serial order in behavior. *Cerebral Mechanisms in Behavior*, LA Jeffress, ed.

McCutcheon, R. A., Abi-Dargham, A., & Howes, O. D. (2019). Schizophrenia, Dopamine and the Striatum: From Biology to Symptoms. *Trends Neurosci, 42*(3), 205-220. doi:10.1016/j.tins.2018.12.004

Miall, R. C., & Wolpert, D. M. (1996). Forward models for physiological motor control. *Neural Networks, 9*(8), 1265-1279. doi:Doi 10.1016/S0893-6080(96)00035-4

Miller, G. A. (1956). The magical number seven plus or minus two: some limits on our capacity for processing information. *Psychol Rev, 63*(2), 81-97. Retrieved from https://www.ncbi.nlm.nih.gov/pubmed/13310704

Murphy, K., James, L. S., Sakata, J. T., & Prather, J. F. (2017). Advantages of comparative studies in songbirds to understand the neural basis of sensorimotor integration. *J Neurophysiol, 118*(2), 800-816. doi:10.1152/jn.00623.2016

Pfordresher, P. Q., & Beasley, R. T. (2014). Making and monitoring errors based on altered auditory feedback. *Front Psychol, 5*, 914. doi:10.3389/fpsyg.2014.00914

Postmes, L., Sno, H. N., Goedhart, S., van der Stel, J., Heering, H. D., & de Haand, L. (2014). Schizophrenia as a self-disorder due to perceptual incoherence. *Schizophrenia Research, 152*(1), 41-50. doi:10.1016/j.schres.2013.07.027

Pruitt, T. A., & Pfordresher, P. Q. (2015). The role of auditory feedback in speech and song. *J Exp Psychol Hum Percept Perform, 41*(1), 152-166. doi:10.1037/a0038285

Ryalls, J. (1994). Postlingually Acquired Deafness - Speech Deterioration and the Wider Consequences - Trends in Linguistics Studies Monograph-62 - Cowie,R, Douglascowie,E. *Canadian Journal of Linguistics-Revue Canadienne De Linguistique, 39*(4), 366-368. doi:Doi 10.1017/S0008413100015577

Sakai, K., Kitaguchi, K., & Hikosaka, O. (2003). Chunking during human visuomotor sequence learning. *Exp Brain Res, 152*(2), 229-242. doi:10.1007/s00221-003-1548-8

Schneider, D. M., & Mooney, R. (2018). How Movement Modulates Hearing. *Annual Review of Neuroscience, Vol 41, 41*, 553-572. doi:10.1146/annurev-neuro-072116-031215

Schneider, D. M., Nelson, A., & Mooney, R. (2014). A synaptic and circuit basis for corollary discharge in the auditory cortex. *Nature, 513*(7517), 189-194. doi:10.1038/nature13724

Schneider, D. M., Sundararajan, J., & Mooney, R. (2018). A cortical filter that learns to suppress the acoustic consequences of movement. *Nature, 561*(7723), 391-395. doi:10.1038/s41586-018-0520-5

Seal, M. L., Aleman, A., & McGuire, P. K. (2004). Compelling imagery, unanticipated speech and deceptive memory: neurocognitive models of auditory verbal hallucinations in schizophrenia. *Cogn Neuropsychiatry, 9*(1-2), 43-72. doi:10.1080/13546800344000156

Selected-Writings of Jackson, John, Hughlings - Taylor,J. (1958). *Psychiatric Quarterly, 32*(3), 614-615. Retrieved from <Go to ISI>://WOS:A1958CGQ9500050

Shepherd, G. M. (2013). Corticostriatal connectivity and its role in disease. *Nat Rev Neurosci, 14*(4), 278-291. doi:10.1038/nrn3469

Shergill, S. S., Samson, G., Bays, P. M., Frith, C. D., & Wolpert, D. M. (2005). Evidence for sensory prediction deficits in schizophrenia. *Am J Psychiatry, 162*(12), 2384-2386. doi:10.1176/appi.ajp.162.12.2384

Sperry, R. W. (1950a). Neural basis of the spontaneous optokinetic response produced by visual inversion. *J Comp Physiol Psychol, 43*(6), 482-489. doi:10.1037/h0055479

Sperry, R. W. (1950b). Neural Basis of the Spontaneous Optokinetic Response Produced by Visual Inversion. *Journal of Comparative and Physiological Psychology, 43*(6), 482-489. doi:DOI 10.1037/h0055479

Subramanian, D., Alers, A., & Sommer, M. A. (2019). Corollary Discharge for Action and Cognition. *Biol Psychiatry Cogn Neurosci Neuroimaging, 4*(9), 782-790. doi:10.1016/j.bpsc.2019.05.010

Tecuapetla, F., Jin, X., Lima, S. Q., & Costa, R. M. (2016). Complementary Contributions of Striatal Projection Pathways to Action Initiation and Execution. *Cell, 166*(3), 703-715. doi:10.1016/j.cell.2016.06.032

Thakkar, K. N., & Rolfs, M. (2019). Disrupted Corollary Discharge in Schizophrenia: Evidence From the Oculomotor System. *Biol Psychiatry Cogn Neurosci Neuroimaging, 4*(9), 773-781. doi:10.1016/j.bpsc.2019.03.009

Tsakiris, M., Schutz-Bosbach, S., & Gallagher, S. (2007). On agency and body-ownership: phenomenological and neurocognitive reflections. *Conscious Cogn, 16*(3), 645-660. doi:10.1016/j.concog.2007.05.012

Vonholst, E., & Mittelstaedt, H. (1950). Das Reafferenzprinzip - (Wechselwirkungen Zwischen Zentralnervensystem Und Peripherie). *Naturwissenschaften, 37*(20), 464-476. doi:Doi 10.1007/Bf00622503

Weiss, C., Herwig, A., & Schutz-Bosbach, S. (2011). The self in action effects: selective attenuation of self-generated sounds. *Cognition, 121*(2), 207-218. doi:10.1016/j.cognition.2011.06.011

Wolpert, D. M., Ghahramani, Z., & Jordan, M. I. (1995). An internal model for sensorimotor integration. *Science, 269*(5232), 1880-1882. doi:10.1126/science.7569931

Wymbs, N. F., Bassett, D. S., Mucha, P. J., Porter, M. A., & Grafton, S. T. (2012). Differential recruitment of the sensorimotor putamen and frontoparietal cortex during motor chunking in humans. *Neuron, 74*(5), 936-946. doi:10.1016/j.neuron.2012.03.038

Zhang, Q., Zhou, X. H., Li, Y. J., Yang, X. D., & Abbasi, Q. H. (2021). Clinical Recognition of Sensory Ataxia and Cerebellar Ataxia. *Frontiers in Human Neuroscience, 15*. doi:ARTN 63987110.3389/fnhum.2021.639871

Zimmermann, G., Brown, C., Kelso, J. A. S., Hurtig, R., & Forrest, K. (1988). The Association between Acoustic and Articulatory Events in a Delayed Auditory-Feedback Paradigm. *Journal of Phonetics, 16*(4), 437-451. doi:Doi 10.1016/S0095-4470(19)30520-0

Chapter 2: Auditory feedback-assisted action sequence task

2.1 Task design

To investigate the role of sensory feedback in action control, we designed a task in which mice learned to perform a heterogeneous action sequence with the help of discriminative auditory feedback (Figure 1A). Briefly, in an operant chamber, trials began with simultaneous extension of left and right levers, and after mice made four lever presses, both levers retracted. Among all possible four-press sequences, only the ‘‘left-left-right-right’’ (LLRR) sequence would be rewarded. Throughout the task, discriminative auditory feedback was provided: each left or right lever press was followed by a 3kHz or 8 kHz pure tone feedback, respectively. In untrained mice, the pattern of lever presses was disorganized and consisted of predominantly right lever presses. With training, mice gradually acquired the target LLRR sequence and performed it with a highly coordinated spatiotemporal pattern (Figure 1B).

2.1 Learning

The mice’s performance efficiency significantly increased following training. Both groups eventually reached the same level of efficiency by the end of the second week (Figure 1C). However, the mice receiving auditory feedback learned significantly better in the early phase of training, in comparison to the controls that learned the same action sequence without

auditory feedback (Figure 1D). A closer examination on the sequence structure across training revealed that the animal firstly identified the final RR, followed by the first L and lastly the second L. In other words, animals can grasp the pattern ‘‘L – RR’’ relatively early, whereas the second element is the most difficult one to acquire. There is an inclination toward a premature switch from L to R (“LRRR”) in the mice, and the determining factor to master the task is the capability to correctly select the second element as a L press. Providing mice with auditory feedback significantly increases the correctness of this critical second element of the sequence during early learning (Figure 1E). In well-trained mice, their performance efficiency significantly dropped without proper auditory feedback provided (Figure 1F). Taken together, these data indicate that auditory feedback is sufficient to enhance action sequence learning and is utilized by mice during the execution of the learned sequence.

2.3 Manipulation of auditory feedback

To further confirm that auditory feedback can really modulate behavioral choice and assist in deciding the optimal timing of switching between LL and RR subsequences, we introduced tone perturbation to well-trained mice for whom auditory feedback was highly predictable. In this experiment, we tested mice trained in the task with probe trials in which the anticipated tone following the first left, second left, or first right lever press was omitted during sequence execution. To mice, lack of expected auditory feedback might indicate an unsuccessful attempt of an action. If this was true, the animals would tend to repeat the same action. Indeed, we found that omission of auditory feedback of the first or second left lever

press facilitated ongoing actions – the likelihood to select the left lever press as the succeeding action significantly increased (Figure 2A and B). Omission of auditory feedback of the first right lever press did not change action selection at the final position of the sequence, indicating state-dependent modulatory effects of auditory feedback. This result was not surprising because the probability of pressing right again following "LLR" in trained mice is normally nearly 100%. Following the same logic, we next tested whether inserting an additional tone associated with a future element of the sequence could also alter mice's action selection. In this case, we predicted that mice might 'skip' that future element and 'jump' onto the next succeeding element of the sequence, due to a false belief that they had already fulfilled a future action. Interestingly, we did observe that following the first left press and the associated auditory feedback, delivering 'future' auditory feedback of the second left press elicited an early behavioral switch – mice were more prone to skipping left lever presses and switching to the right at the second position of the sequence (Figure 2C). Similarly, inserting the "future" auditory feedback of the first right presses further increased the likelihood of pressing right at the third position of the sequence (Figure 2D). As expected, inserting the tone associated with the second right lever press did not change action selection for the final position of the sequence. All together these results show that alteration of auditory feedback can modulate online action selection and auditory feedback is crucial for guiding behavioral switching.

Part of chapter 2 is currently being prepared for submission for publication of the material. (Huang, Hsiang-Hsuan; Yan, Xunyi; Zhang, Baibing; Jin, Xin.) The dissertation author was the primary researcher and author of this material.

Figure 1. Auditory feedback facilitates action sequence learning and is involved in action sequence execution

(A) Operant chamber schematic. Artificial auditory feedback for distinguishing left versus right lever press is provided when mice perform the LLRR sequence task.

(B) Example of typical wild-type mouse behavior on day 1 (left) and day 14 (right) of training. Top panels: left and right lever presses indicated by blue and red dashes, respectively, and aligned to the final lever press at time zero. Bottom panels: averaged left- and right-lever pressing rate indicated by blue and red lines, respectively.

(C) Behavioral efficiency for mice trained with the auditory feedback-assisted task (L3kR8k, n=12) versus mice trained with no tone version of the task (Control, n=10) across 14 days of training (main effect of training: $F_{3,60}$ =49.82, p<0.0001; main effect of auditory feedback: $F_{1, 20}$=3.402, p=0.0800).

(D) Behavioral efficiency for mice trained with auditory feedback-assisted task (L3kR8k, n=20) versus mice trained with no tone version of the task (Control, n=15) across 7 days of training. (main effect of training: $F_{4.130, 136.3}$ = 88.06, p<0.0001; main effect of auditory feedback: $F_{1, 33}$ =7.174, p=0.0114).

(E) Percentage of sequences containing each appropriate element position for mice trained with auditory feedback and no tone control across training. (- L - -: main effect of training: $F_{6, 198}$ = 13.94, p<0.0001; main effect of auditory feedback: $F_{1, 33}$=4.396, p=0.0438).

(F) Behavioral efficiency for mice trained with auditory feedback (n=8) decreased when tone was canceled at each lever press with a 50% probability in randomly selected 15% of total trials (paired t-test, t_7=4.216, p=0.0040).

Data were analyzed using repeated-measures two-way ANOVA if not else mentioned. Error bars denote SEM.

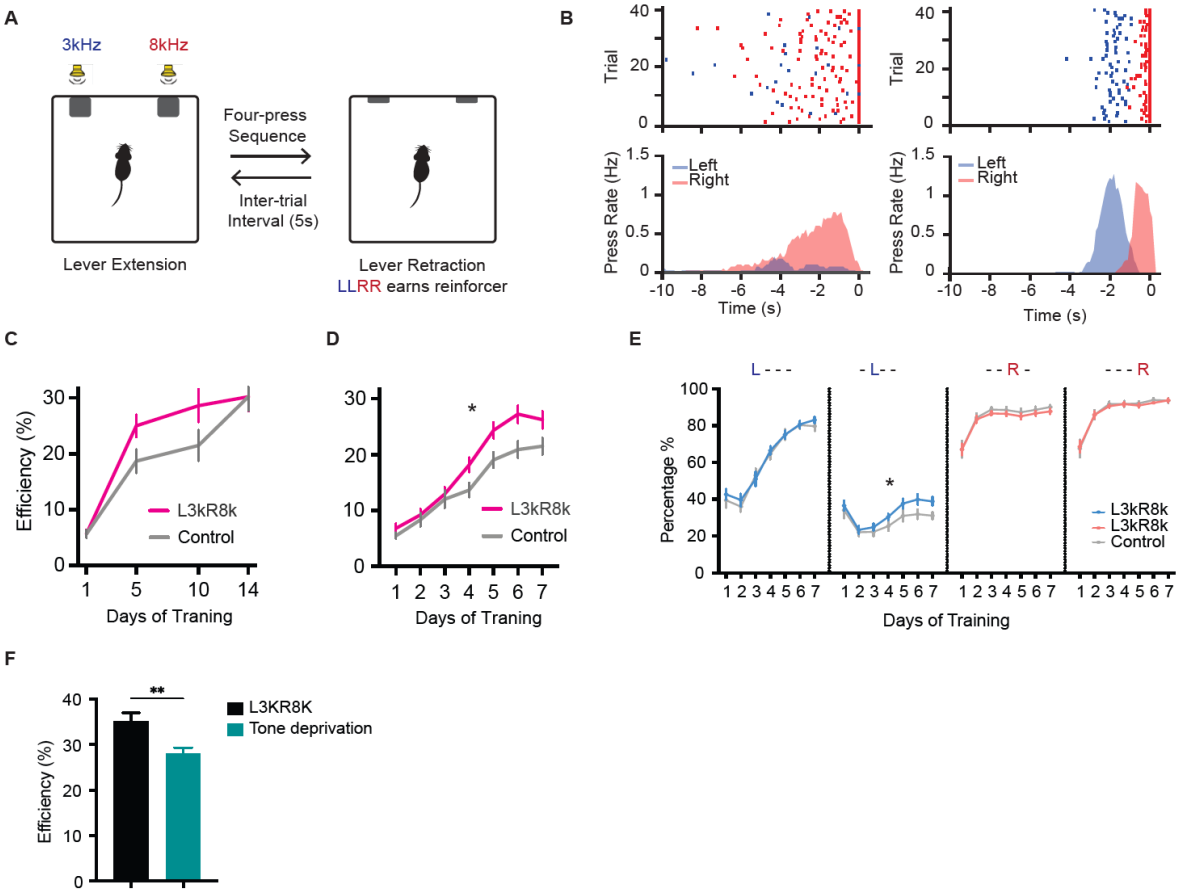
A
3kHz
8kHz
Four-press
Sequence
Inter-trial
Interval (5s)
Lever Extension
Lever Retraction
LLRR earns reinforcer
B
Trial
Press Rate (Hz)
Left
Right
Time (s)
C
Efficiency (%)
L3kR8k
Control
Days of Traning
D
*
L3kR8k
Control
Days of Traning
E
L - - -
- L - -
- - R -
- - - R
Percentage %
*
L3kR8k
L3kR8k
Control
Days of Training
F
**
L3KR8K
Tone deprivation
Efficiency (%)

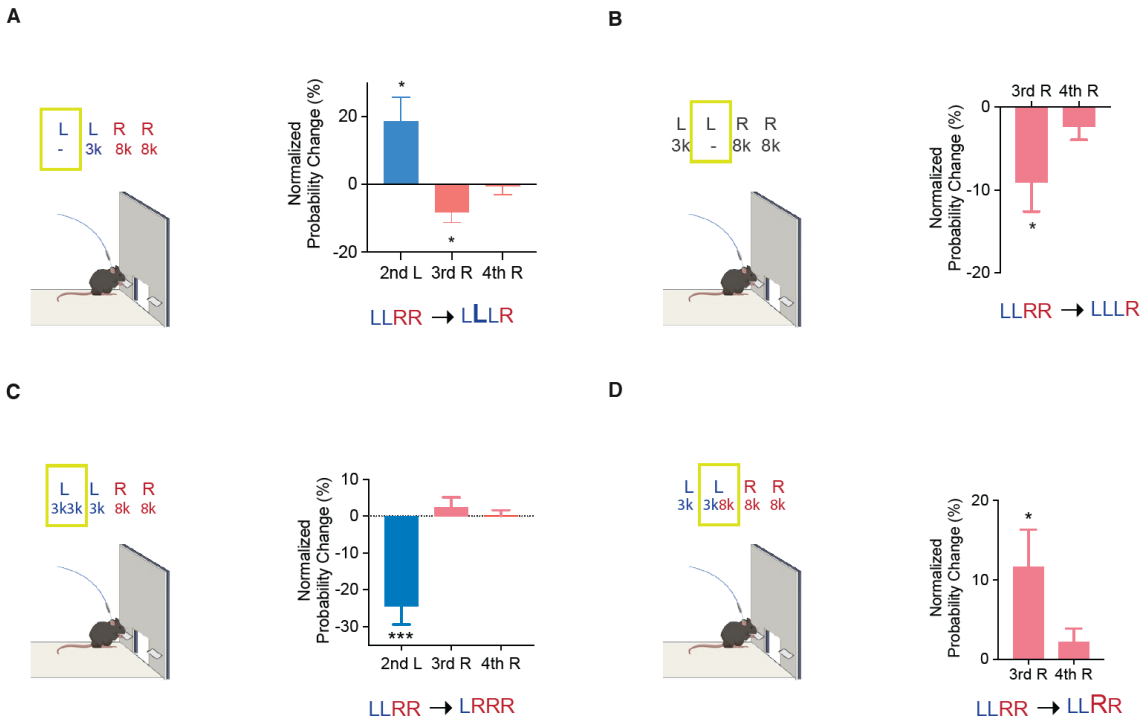

Figure 2. Auditory feedback is critical for the proper switch between action subsequences

(A and B) Omitting artificial auditory feedback of the first (A) or second (B) left press within the sequence in randomly selected probe trials when the mice performed the tone-assisted task. The bar graphs indicate normalized changes in probability for the succeeding elements to be a left press (2^{nd} L), a right press (3^{rd} R), and another right press (4^{th} R) subsequently, following manipulation of the tone on the first left press (A) or the second left press (B) (A: n=7, 2nd L: paired t-test, t_6=2.660, p=0.0375; F, 3rd R: paired t-test, t_6=2.885, p=0.0290. B: n=7, 3rd R: paired t-test, t_6=2.627, p=0.0392).

(C-D) Inserting artificial auditory feedback associated with the next element within the target sequence (LLRR) when the mice made the first (C) or second left (D) press in randomly chosen probe trials. The bar graphs indicate normalized changes in probability for the succeeding elements to be a left press (2^{nd} L), a right press (3^{rd} R), and a right press (4^{th} R) subsequently, following manipulation of the tone in (C) and (D).

(C: n=10, 2nd L: paired t-test, t_9=5.138, p=0.0006. D: n=8, 3rd R: paired t-test, t_7=2.737, p=0.0290). Error bars denote SEM.

.

Chapter 3: The neural substrate for integrating sensorimotor feedback

3.1 Auditory cortex is essential for transducing task-related sensory feedback

To address the role of the auditory cortex in the implementation of auditory feedback-assisted sequence execution, we first assessed the expression of the immediate early gene c-Fos, a marker widely used to visualize activated neurons in the brain, following the training. After the mice performed the task, we perfused the brain and conducted immunohistochemistry for c-Fos. There was robust c-Fos expression present in the auditory cortex (Figure 3A). We next tested whether neuronal activity in the auditory cortex is required for performing the task. Inactivation of the auditory cortex with bilateral infusion of muscimol, a selective $GABA_A$ agonist, significantly impaired task performance (Figure 3B), suggesting auditory input is indispensable for executing the learned action sequence. This raises the possibility that mice could not organize the learned sequence well because the processing of auditory feedback is disrupted. To test this idea, we sought to use optogenetics to inhibit the auditory cortex more precisely over a narrow time window around the auditory feedback delivery. We found that optogenetically inhibiting the auditory cortex following the first or second left lever press resulted in an increased probability of selecting the left lever press as the succeeding action (Figure 3C and D). These results recapitulate the behavioral effects elicited by naturally omitting the expected auditory feedback (Figure 2A and B). Previously we have shown inserting additional auditory tones was sufficient to alter mice's action selection (Figure 2C and D). These behavioral changes were abolished by optogenetic inhibition of the auditory cortex during the tone delivery (Figure 3E and F), indicating its role

in transmitting moment-to-moment sensory information essential for task performing. Taken together, these results confirm the auditory cortex is necessary for transducing auditory feedback to control action sequence implementation.

3.2 Optogenetics screening for integration centers

We next sought to identify the brain regions that may integrate auditory-motor feedback to achieve action sequence control. To this end, we performed anterograde tracing by injecting AAV-CAG-tdTomato into the auditory cortex and found that several cortical regions receive abundant afferents, including the cingulate cortex (Cg), the secondary motor cortex (M2), posterior parietal cortex (PPC) and orbitofrontal cortex (OFC) (Figure 4A). Through screening with optogenetic inhibition, we revelated that the cingulate cortex and the medial portion of M2 (Cg/M2) is a potential sensorimotor integration center, given that suppressing Cg/M2 activity following the animals performing the first or second left lever press resulted in a robust increase in the probability of repeating the ongoing action and thus delayed between-subsequence switching (Figure 4C-H). In addition, we showed that inactivation of Cg/M2 with bilateral infusion of muscimol largely compromised mice's task efficiency (Figure 4B), suggesting it is indispensable for appropriate sequence organization. To first determine whether Cg/M2 is a critical node that integrates auditory inputs, we utilized designer receptors exclusively activated by designer drugs (DREADDs) to specifically silence auditory cortex– Cg/M2 projections. We found that inhibition of this pathway significantly impaired task performance (Figure 5B), supporting the idea Cg/M2 is important for

integrating auditory feedback information. Moreover, this pathway seems to be essential specifically for the discriminative auditory feedback, rather than lever-pressing sounds (Figure 5D). Taken together, these results indicate that the capability of integrating moment-to-moment sensorimotor feedback underlies the mechanism by which Cg/M2 dictates action sequence execution.

Part of chapter 3 is currently being prepared for submission for publication of the material. (Huang, Hsiang-Hsuan; Yan, Xunyi; Zhang, Baibing; Jin, Xin.) The dissertation author was the primary researcher and author of this material.

Figure 3. Optogenetic inhibition of the auditory cortex blocks sensory feedback
(A) c-Fos induction in auditory cortex of trained mice following auditory feedback assisted sequence task.
(B) Inhibition of the auditory cortex with muscimol during the task. The line chart indicates behavioral efficiency of performance in trained mice during the muscimol infusion day and the pre-/post-control days (n=7, pre-control versus muscimol: paired t-test: t_6=2.832, p=0.029).
(C and D) Optogenetic inhibition (by stimulating inhibitory interneurons in the auditory cortex) following the first (C) or the second left (D) press of the sequence when the trained Vgat-Ai32 mice performed auditory feedback assisted task. 500-ms 473nm light was delivered triggered by the selected lever presses within the sequence, in randomly chosen probe trials. The bar graphs indicate normalized changes in probability for the succeeding elements to be a left press (2^{nd} L), a right press (3^{rd} R), and a right press (4^{th} R) subsequently, following optogenetic inhibition on the first left (D) and the second left press (D) (C: n=10, 2nd L: paired t-test, t_9=6.030, p=0.0003. D: n=7, 3rd R: paired t-test, t_6=4.440, p=0.044).
(E and F) Optogenetic inhibition (by stimulating inhibitory interneurons in the auditory cortex) during an additional tone associated with the next element within the target sequence (LLRR) when the mice made the first (E) or second left (F) press in randomly chosen probe trials. 175-ms 473nm light was delivered triggered by the selected lever presses within the sequence to cover the duration of the additional tone. The bar graphs indicate normalized changes in probability for the succeeding elements to be a left press (2^{nd} L), a right press (3^{rd} R), and a right press (4^{th} R) subsequently, following optogenetic manipulation (F: n=4, 3rd R: paired t-test, t_3=1.103, p=0.3505). Error bars denote SEM.

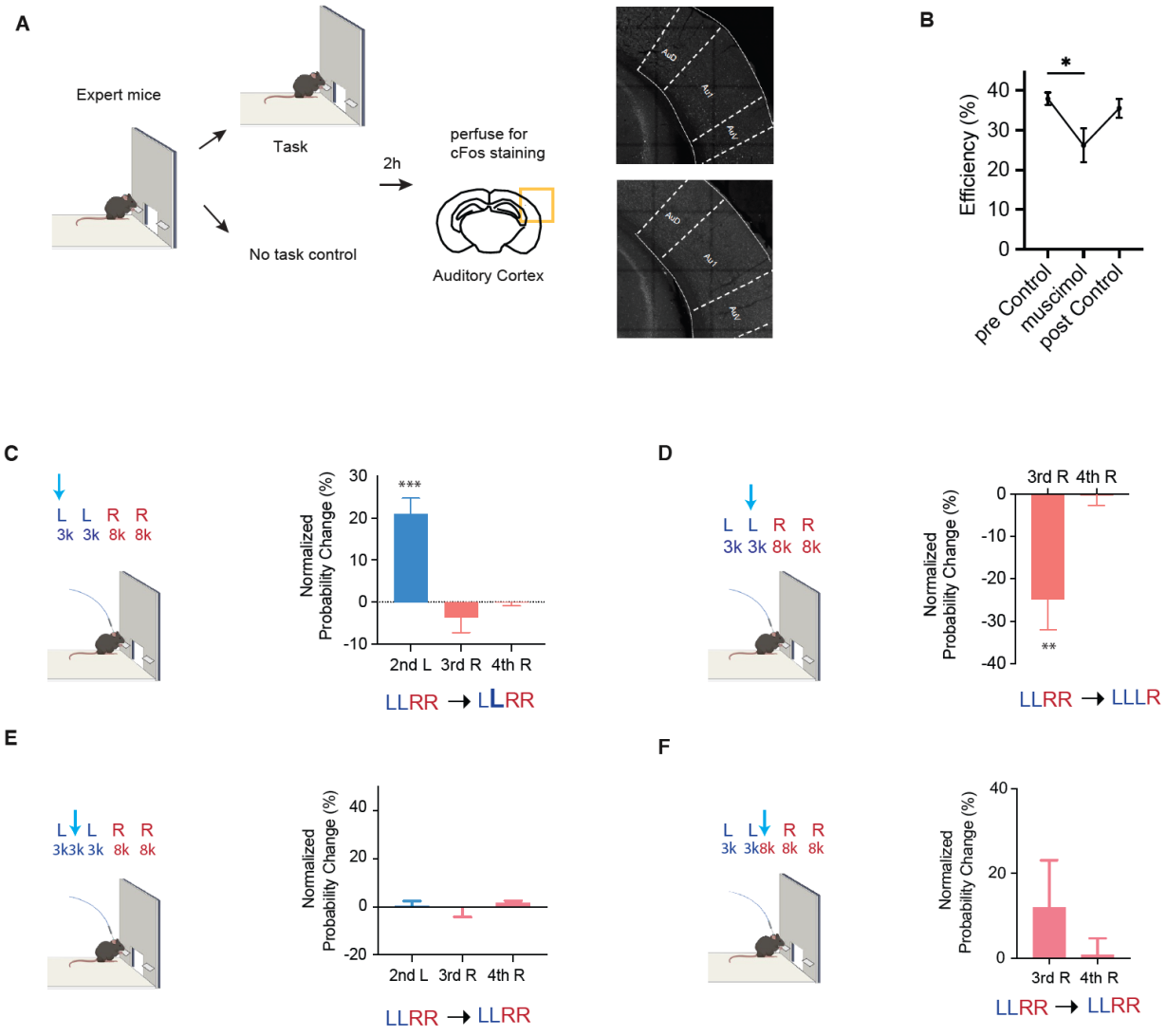
A
Expert mice
Task
No task control
2h
perfuse for
cFos staining
Auditory Cortex
AuD
Au1
AuV
B
Efficiency (%)
40
30
20
10
0
*
pre Control
muscimol
post Control
C
L L R R
3k 3k 8k 8k
Normalized
Probability Change (%)
30
20
10
0
-10
***
2nd L 3rd R 4th R
LLRR → LLRR
D
L L R R
3k 3k 8k 8k
3rd R 4th R
0
-10
-20
-30
-40
**
LLRR → LLLR
E
L L R R
3k 3k 3k 8k 8k
40
20
0
-20
2nd L 3rd R 4th R
LLRR → LLRR
F
L L R R
3k 3k 8k 8k 8k
40
20
0
3rd R 4th R
LLRR → LLRR

Figure 4. Optogenetic inhibition of Cg/M2 delays between-subsequence switch
(A) Anterograde tracing from the auditory cortex to screen the candidates of the cortical regions receiving auditory feedback information. The injection site was validated by the abundant innervation in the medial geniculate nucleus (MGN) of the thalamus and the posterior striatum.
(B) Inhibition of Cg/M2 with muscimol during the task. The line chart indicates behavioral efficiency of performance in trained mice during the muscimol infusion day and the pre-/post-control (n=8, pre-control versus muscimol: paired t-test: t_7=4.620, p=0.0024).
(C-H) Optogenetic inhibition (by stimulating inhibitory interneurons in Cg/M2) following the first (C) or the second left (F) press of the sequence when the trained Vgat Ai32 mice performed the auditory feedback-assisted task. 500-ms 473nm light was delivered triggered by the selected lever presses within the sequence, in randomly chosen probe trials.
(D and G) Behavioral examples of Cg/M2 inhibition in (C) and (F), respectively. Left panels: control trials. Right panels: probe trials. Grey shadow indicates the duration of laser delivery.
(E and H) The bar graphs indicate normalized changes in probability for the succeeding elements to be a left press (2^{nd} L), a right press (3^{rd} R), and a right press (4^{th} R) subsequently, following optogenetic inhibition on the first left (F) or the second left press (I).
(E: n=8, 2nd L: paired t-test, t_7=4.155, p=0.0043; 3rd R: paired t-test, t_7=5, p=0.0616. I: n=7, 3rd R: paired t-test, t_6=4.059, p=0.0067)
(I-N) Optogenetic inhibition (by stimulating inhibitory interneurons in Cg/M2) during an additional tone associated with the next element within the target sequence (LLRR) when the mice make the first (I) or second left (L) presses in randomly chosen probe trials. 175-ms 473nm light was delivered triggered by the selected lever presses within the sequence to cover the duration of the additional tone.
(J and M) Behavioral examples of Cg/M2 inhibition in (I) and (L), respectively.
(K and N) The bar graphs indicate normalized changes in probability for the succeeding elements to be a left press (2^{nd} L), a right press (3^{rd} R), and a right press (4^{th} R) subsequently, following optogenetic manipulation. (N: n=5, 3rd R: paired t-test, t_4=3.669, p=0.0214.)
Error bars denote SEM.

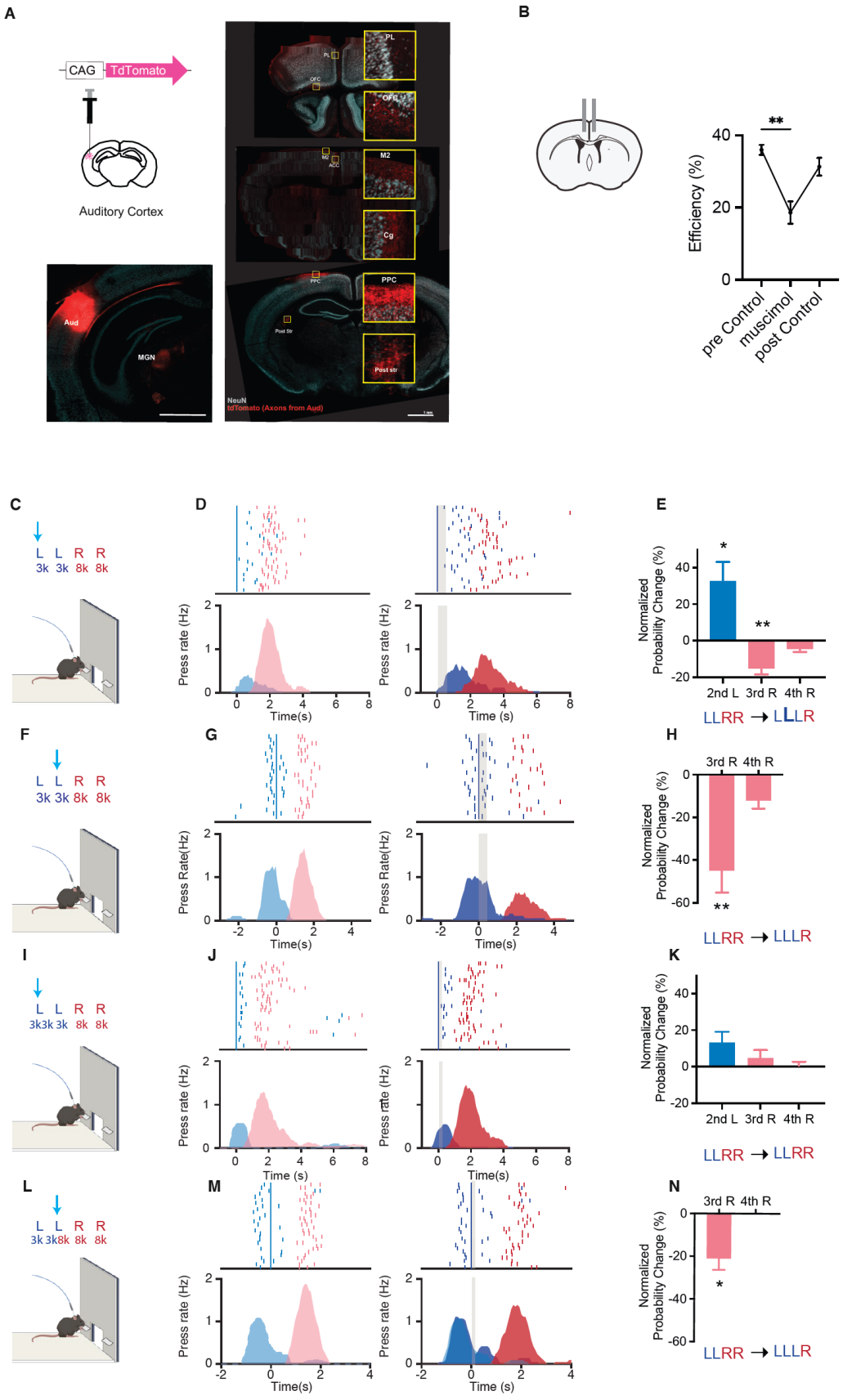
A
CAG
TdTomato
Auditory Cortex
PL
OFC
M2
Cg
PPC
Post str
Aud
MGN
NeuN
tdTomato (Axons from Aud)
B
Efficiency (%)
40
20
0
**
pre Control
muscimol
post Control
C
L L R R
3k 3k 8k 8k
D
Press rate (Hz)
Time(s)
Time (s)
E
Normalized Probability Change (%)
2nd L 3rd R 4th R
LLRR → LLLR
F
G
Press Rate(Hz)
H
3rd R 4th R
I
3k3k 3k 8k 8k
J
K
2nd L 3rd R 4th R
LLRR → LLRR
L
3k 3k8k 8k 8k
M
N
3rd R 4th R
LLRR → LLLR

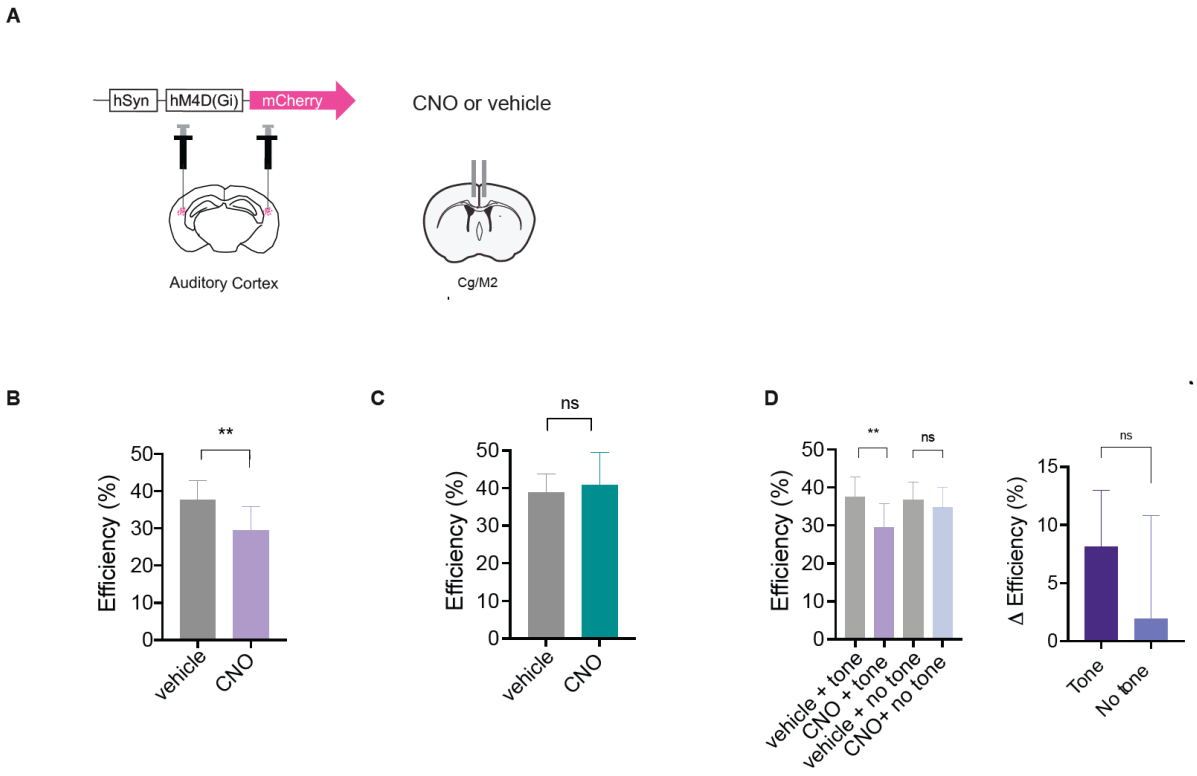

Figure 5. Chemogenetic silencing of auditory cortex to Cg/M2 projection attenuates auditory feedback-assisted sequence performance

(A) Schematic representing injection of AAV-hSyn-hMD4(Gi)-mCherry into the bilateral auditory cortex and CNO infusion into Cg/M2 via implanted cannulas.

(B) Behavioral efficiency of trained mice injected with inhibitory Gi DREADDs on the day infused with CNO versus on the day infused with vehicle, 30 minutes prior to the session of auditory feedback-assisted task (n=6, paired t-test, t_5=4.040, p=0.0099).

(C) Behavioral efficiency of trained mice injected with AAV carrying only fluorescent proteins (as control) on the day infused with CNO and on the day infused with vehicle, 30 minutes prior to the session of auditory feedback-assisted task (n=5, paired t-test, t_4=0.9005, p=0.4188).

(D) Comparison of inhibitory effects in the mice in (B) performing the auditory feedback-assisted task or the no-tone version of the action sequence task.

Error bars denote SEM.

.

Chapter 4: Dual corticostriatal circuits for controlling action sequence

4.1 Cg/M2-DMS pathway controls subsequence switch

Previously, the striatal direct and indirect pathways have been shown to coordinatively control action sequencing, and the latter selectively guides between-subsequence switch (Geddes et al., 2018). The Dorsomedial striatum (DMS) receives abundant innervation from Cg/M2. Together with our findings that inhibiting Cg/M2 prevented the animal from switching (Figure 4C-H), it is possible that Cg/M2 regulates subsequence switch through its projections to DMS. To test this idea, we next sought to investigate whether activation of the Cg/M2–DMS pathway is sufficient to trigger a behavioral switch. To do this, we injected retrograde adeno-associated viral (AAV) vector carrying FlpO recombinase (AAVRetro-FlpO) into the DMS and FlpO-dependent channelrhodopsin-2 (AAV-fDIO-ChR2-eYFP) into Cg/M2 to selectively label DMS-projecting neurons in Cg/M2 (Figure 6A left). We found that optogenetically stimulating Cg/M2 neurons projecting to DMS following the first or second left lever press significantly increased the probability of halting the ongoing action and switching to the right lever (Figure 6B-G). Similarly, optogenetically stimulating Cg/M2→DMS terminals (Figure 6A right) produced the same behavioral effects (Figure 6H-M). These findings thus further confirm the essential role of Cg/M2 in mediating subsequence switch through corticocortical pathways.

4.2 In vivo electrophysiological recording of Cg/M2

We next moved to investigate the neural activities in Cg/M2 during auditory feedback-assisted action sequencing by in vivo electrophysiological recordings. Intriguingly, we identified a portion of Cg/M2 neurons that are exclusively active during the transition from the left to the right subsequences (Figure 7 A and B). This 'switch-related activity emerged after the second left press and terminated before the first right press and spanned throughout the transition period. Similar switch-related activity has previously been observed in D2-expressing (indirect pathway) spiny projection neurons (iSPNs) in the striatum (Geddes et al. 2018). Moreover, we also identified Cg/M2 neurons responsive to altered auditory feedback, which can be categorized into two groups (Figure 7C). 31% of these neurons are 'sensory neurons', whose activity increased faithfully in response to auditory tones (Figure 7D and E). In contrast, 69% of these neurons did not respond to auditory tones themselves but showed phasic activity selectively to unexpected auditory feedback and were therefore termed "prediction error neurons". The presence of prediction error neurons indicates that Cg/M2 receives motor representation signaling self-generated action. These results collectively support the role of Cg/M2 in sensorimotor integration and guiding behavioral switching.

4.3 Slice electrophysiological recording of dSPN vs. iSPN to Cg/M2–DMS stimulation

Striatal iSPNs have been shown to mediate subsequence switch (Geddes et al. 2018). This raises the possibility that the behavioral switch driven by stimulating the Cg/M2–DMS pathway (Figure 6H-M) can be attributed to the activation of iSPNs. To test this idea, we examined the postsynaptic responses of dSPNs versus iSPNs in DMS to Cg/M2 inputs excitation. Here, we conducted ex vivo patch-clamp recordings in pairs of adjacent striatal

dSPNs and iSPNs, while optogenetically stimulating Cg/M2 terminals in proximity (Figure 8A). Noticeably, we observed larger EPSCs in iSPNs in almost all pairs of neurons (Figures 8C and D). There were no differences in the paired-pulse ratio (PPR) (Figure 8E). These results suggest that Cg/M2 preferentially innervates iSPNs in DMS and Cg/M2 may mediate behavioral switching through activation of iSPNs.

4.4 M1–DLS pathway facilitates ongoing actions

To identify the possible sources of motor representation, we sought to investigate whether the primary motor cortex (M1) is involved in auditory feedback-assisted sequence execution. We found that inhibition of M1 following the first left lever press resulted in an increased probability of premature switching to the right lever (Figure 9A), suggesting that M1 may be involved in promoting ongoing actions. M1 primarily innervates the dorsolateral striatum (DLS), and it is possible M1 controls action sequencing through its projection to DLS. To further test this idea, we next tested the behavioral effects of optogenetic stimulation of the M1–DLS pathway. As expected, activation of DLS-projecting M1 neurons when the animals pressed the first left lever generated effects opposite to M1 inhibition (Figure 9C). Moreover, activation of M1→DLS terminals following the first or second left press also facilitated ongoing actions and increasingly inserted an additional left press before switching (Figures 9E and F). It has been previously shown striatal D1-expressing direct pathway spiny projection neurons (dSPNs) facilitate actions and encode sequence start/stop (Geddes et al. 2018). Slice electrophysiology further revealed that M1 preferentially innervates dSPNs in

DLS (Figure S6) and it is possible that M1 promotes action via dSPNs activation. Together these results imply M1–DLS pathway facilitates ongoing actions and might be the source of motor representation conveying to Cg/M2. Chemogenetic inhibition of M1 terminals in Cg/M2 interfered with action sequence execution (Figure S5). This result suggests M1–Cg/M2 projection is one route through which motor signals are transmitted.

4.5 Model of dual corticostriatal pathways controlling sensory feedback-guided action sequencing

To summarize, the experimental data of the present study suggest there are two parallel corticostriatal pathways that dynamically coordinate their activity in controlling action sequence execution. Based on our results, we came up with a model to account for the roles of these two pathways. The M1–DLS pathway is responsible for the facilitation of elemental actions, through the striatal direct pathways, whereas the Cg/M2–DMS pathway inhibits actions and mediates subsequence switch through the indirect pathway. It is possible the M1–DLS pathway is first activated to start the action sequence and continue to promote actions. The auditory feedback and motor representation of lever pressing would be transmitted to and integrated in Cg/M2. The presence of both motor representation and the compatible sensory feedback indicates an action is performed properly and possibly increases Cg/M2 activity. Upon finishing the first subsequence, Cg/M2–DMS is now more active than the M1–DLS pathway and takes over the control, halting the current action and triggering a switch to the second subsequence. This model also helps to explain why inhibition of the

auditory cortex and Cg/M2 following the first or second left press, the animals are more likely to repeat a left press, while inhibition of M1 instead triggers a behavior switch–because the 'facilitation' pathways would be shut down and the 'switch' pathways would now dominate the system. In a nutshell, this dual pathways model offers a mechanistic explanation for the role of Cg/M2 in sensorimotor integration and actively guiding action sequencing.

Part of chapter 4 is currently being prepared for submission for publication of the material. (Huang, Hsiang-Hsuan; Yan, Xunyi; Zhang, Baibing; Jin, Xin.) The dissertation author was the primary researcher and author of this material.

References

Geddes, C. E., Li, H., & Jin, X. (2018). Optogenetic Editing Reveals the Hierarchical Organization of Learned Action Sequences. *Cell, 174*(1), 32-43 e15. doi:10.1016/j.cell.2018.06.012

Figure 6. Optogenetic stimulation of the Cg/M2–DMS pathway is sufficient to trigger a behavioral switch

(A) Surgical setups and the innervation pattern of corticostriatal inputs from Cg/M2 onto the dorsomedial striatum (DMS). Left panel: striatum-projecting Cg/M2 neurons were expressed with eYFP-tagged ChR2, and optical fibers were implanted in Cg/M2 superficially. Right panel: Cg/M2 neurons were expressed with eYFP-tagged ChR2, and optical fibers were implanted into DMS.

(B–G) Optogenetic stimulation of striatum-projecting Cg/M2 neurons following the first (B) or the second left (E) press of the sequence during auditory feedback-assisted task. 500-ms 473nm light was delivered triggered by the selected lever presses within the sequence, in randomly selected probe trials.

(C and F) Behavioral examples of inhibition of Cg/M2 in (B) and (E), respectively. Left panels: control trials. Right panels: probe trials. Grey shadow indicates the duration of laser delivery.

(D and G) The bar graphs indicate normalized changes in probability for the succeeding elements to be a left press (2^{nd} L), a right press (3^{rd} R), and a right press (4^{th} R) subsequently, following optogenetic stimulation on the first left (B) or the second left press (E). (D: n=8, 2nd L: paired t-test, t_7=4.447, p=0.0029; 3rd R: t_7=4.019, p=0.0051. G: n=6, 3rd R: paired t-test, t_5=4.376, p=0.0072; 4thR: t_5=4.502, p=0.0064)

(H–N) Optogenetic stimulation of Cg/M2 terminals in DMS following the first (H) or the second left (K) press of the sequence during the task. 1-s 473nm light was delivered in randomly selected probe trials.

(I and L) Behavioral examples of Cg/M2 terminal stimulation in (H) and (K), respectively. Left panels: control trials. Right panels: probe trials. Grey shadow indicates the duration of laser delivery.

(J and M) The bar graphs indicate normalized changes in probability for the succeeding elements to be a left press (2^{nd} L), a right press (3^{rd} R), and a right press (4^{th} R) subsequently, following optogenetic stimulation. (J: n=6, 2nd L: paired t-test, t_5=3.265, p=0.0223. M: n=5, 3rd R: paired t-test, t_4=4.822, p=0.0085) Error bars denote SEM.

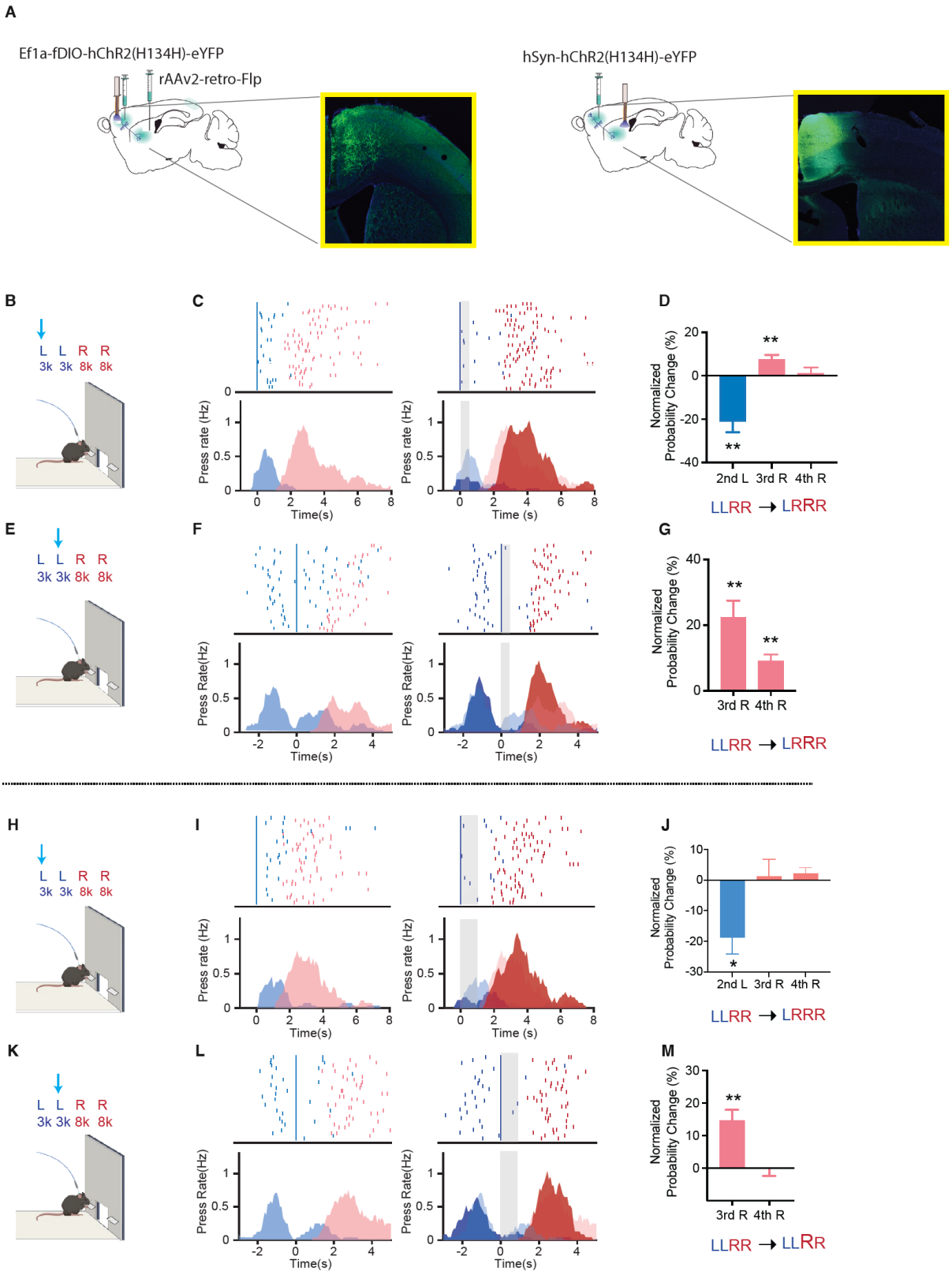
A
Ef1a-fDIO-hChR2(H134H)-eYFP
rAAv2-retro-Flp
hSyn-hChR2(H134H)-eYFP
B
L L R R
3k 3k 8k 8k
C
Press rate (Hz)
Time(s)
Time (s)
D
Normalized Probability Change (%)
2nd L 3rd R 4th R
LLRR → LRRR
E
L L R R
3k 3k 8k 8k
F
Press Rate(Hz)
Time(s)
G
Normalized Probability Change (%)
3rd R 4th R
LLRR → LRRR
H
L L R R
3k 3k 8k 8k
I
Press rate (Hz)
Time(s)
Time (s)
J
Normalized Probability Change (%)
2nd L 3rd R 4th R
LLRR → LRRR
K
L L R R
3k 3k 8k 8k
L
Press Rate(Hz)
Time(s)
M
Normalized Probability Change (%)
3rd R 4th R
LLRR → LLRR

Figure 7. Cg/M2 neurons encode behavioral switch, auditory feedback, and prediction errors in auditory feedback

(A) Representative Cg/M2 neuron exhibiting switch-related activity. Top: each dash in the raster plot indicates a spike. Bottom: neuronal activity is aligned to 50ms before the first left, second left, first right, and second right lever presses within the sequence, respectively.

(B) Peri-event time histogram (PETH) of the same Cg/M2 neuron in (A) with trials sorted by left-to-right subsequence switch intervals. Top panel: each dash indicates a spike. Bottom panel: neuronal activity is aligned to the first right press at time zero.

(C) Distribution of Cg/M2 neurons responsive to altered auditory feedback.

(D) Representative Cg/M2 'sensory' neuron responding to auditory feedback itself. Top panel: each dash indicates a spike. Bottom panel: neuronal activity is aligned to the onset auditory feedback of the first left, second left, first right, and second right lever presses within the sequence, respectively.

(E) Neuronal activity of the same Cg/M2 neuron in (D) in response to altered auditory feedback. Responses to normal auditory feedback (left), omitted auditory feedback (middle left), and unexpected additional auditory feedback (middle right and right) are shown respectively.

(F) Representative Cg/M2 'prediction error' neuron encoding prediction error in auditory feedback. Top panel: each dash indicates a spike. Bottom panel: neuronal activity is aligned to the onset auditory feedback of the first left, second left, first right, and second right lever presses within the sequence, respectively.

(G) Neuronal activity of the same Cg/M2 neuron in (F) in response to altered auditory feedback. Responses to normal auditory feedback (left) and unexpected additional auditory feedback (middle) are shown respectively. This neuron did not respond to 8kHz itself (right).

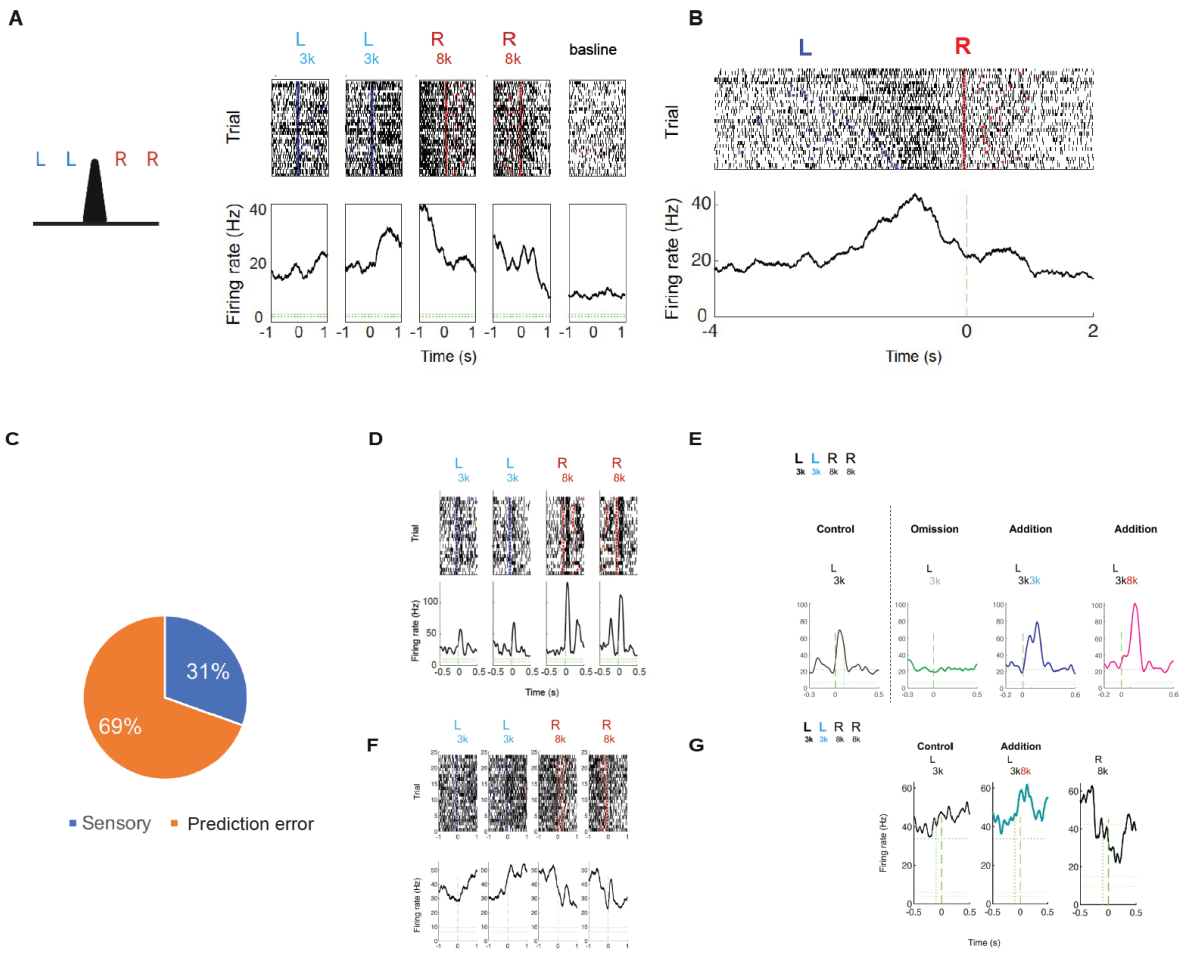
A
L L R R
L 3k
L 3k
R 8k
R 8k
basline
Trial
Firing rate (Hz)
40
20
0
-1 0 1
Time (s)
B
L
R
Trial
Firing rate (Hz)
40
20
0
-4
0
2
Time (s)
C
31%
69%
Sensory
Prediction error
D
L 3k
L 3k
R 8k
R 8k
Trial
Firing rate (Hz)
100
50
0
-0.5 0 0.5
Time (s)
E
L L R R
3k 3k 8k 8k
Control
Omission
Addition
Addition
L 3k
L 3k
L 3k3k
L 3k8k
F
L 3k
L 3k
R 8k
R 8k
Trial
Firing rate (Hz)
G
L L R R
3k 3k 8k 8k
Control
Addition
L 3k
L 3k8k
R 8k
Firing rate (Hz)
60
40
20
0
-0.5 0 0.5
Time (s)

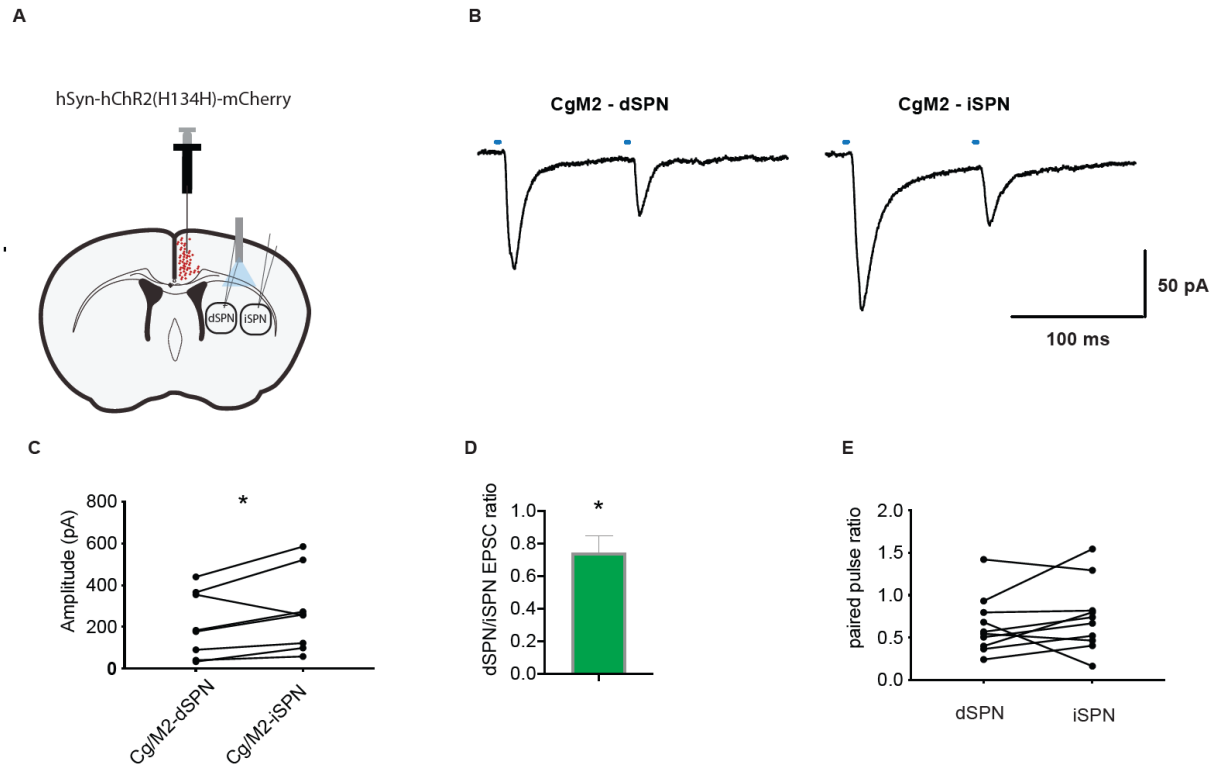

Figure 8. Cg/M2 cortical inputs differentially excite dSPNs vs. iSPNs in DMS
(A)Schematic representation of the experimental setup.
(B) Representative traces of EPSC in a pair of neighboring dSPN and iSPN, in response to optogenetic stimulation of Cg/M2 terminals in DMS.
(C and D) Amplitude (C) and mean ratio (D) of EPSCs in pairs of neighboring dSPNs and iSPNs (n=8) following optogenetic stimulation of Cg/M2 terminals in DMS (ratio paired t-test: t_7=2.662, p= 0.0324).
(E) Paired pulse ratio of the same dSPNs and iSPNs pairs shown in (C and D) following optogenetic stimulation of Cg/M2 terminals in DMS.
Error bars denote SEM.

Figure 9. Optogenetic inhibition of M1 triggers a behavioral switch and stimulation of M1–DLS pathway facilitates ongoing actions

(A and B) Optogenetic inhibition (by stimulating inhibitory interneurons in M1) following the first (A) or the second left (B) press of the sequence when trained Vgat Ai32 mice performed the auditory feedback-assisted task. 500-ms 473nm light was delivered triggered by the selected lever presses within the sequence, in randomly selected probe trials.

The bar graphs indicate normalized changes in probability for the succeeding elements to be a left press (2^{nd} L), a right press (3^{rd} R), and a right press (4^{th} R) subsequently, following optogenetic inhibition on the first left (A) or the second left press (B) (A: n=5, 2nd L: paired t-test, t_4=3.003, p=0.0398. B: n=4, 3rd R: paired t-test, t_3=1.493, p=0.2322).

(C and D) Optogenetic stimulation of striatum-projecting M1 neurons following the first (C) or the second left (D) press of the sequence during the auditory feedback-assisted task. 473nm light was delivered triggered by the selected lever presses within the sequence, in randomly selected probe trials. The bar graphs indicate normalized changes in probability for the succeeding elements to be a left press (2^{nd} L), a right press (3^{rd} R), and a right press (4^{th} R) subsequently, following optogenetic stimulation on the first left (C) or the second left press (D) (C: n=5, 2nd L: paired t-test, t_4=4.018, p=0.0148. D: n=5, 3rd R: paired t-test, t_4=2.0609, p=0.1072).

(E and F) Optogenetic stimulation of M1 terminals in DLS following the first (E) or the second left (F) press of the sequence during the task. 1s 473nm light was delivered in randomly selected probe trials. The bar graphs indicate normalized changes in probability for the succeeding elements to be a left press (2^{nd} L), a right press (3^{rd} R), and a right press (4^{th} R) subsequently, following optogenetic stimulation. (E: n=5, 2nd L: paired t-test, t_4=2.0809, p=0.0446. F: n=5, 3rd R: paired t-test, t_4=3.128, p=0.0353) Error bars denote SEM.

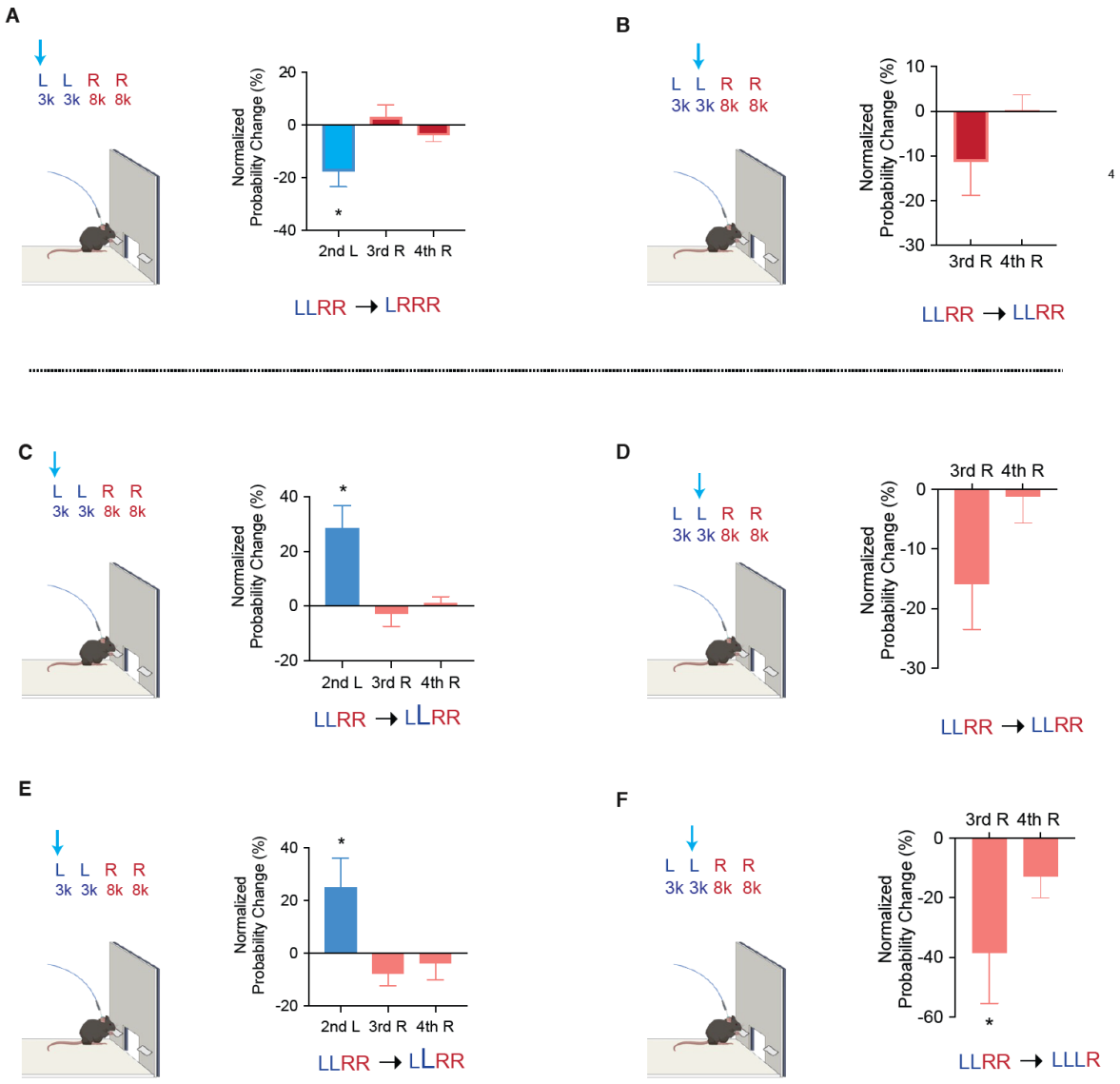
A
L L R R
3k 3k 8k 8k
Normalized Probability Change (%)
20
0
-20
-40
*
2nd L 3rd R 4th R
LLRR → LRRR
B
L L R R
3k 3k 8k 8k
Normalized Probability Change (%)
10
0
-10
-20
-30
3rd R 4th R
LLRR → LLRR
C
L L R R
3k 3k 8k 8k
Normalized Probability Change (%)
40
20
0
-20
*
2nd L 3rd R 4th R
LLRR → LLRR
D
L L R R
3k 3k 8k 8k
3rd R 4th R
Normalized Probability Change (%)
0
-10
-20
-30
LLRR → LLRR
E
L L R R
3k 3k 8k 8k
Normalized Probability Change (%)
40
20
0
-20
*
2nd L 3rd R 4th R
LLRR → LLRR
F
L L R R
3k 3k 8k 8k
3rd R 4th R
Normalized Probability Change (%)
0
-20
-40
-60
*
LLRR → LLLR

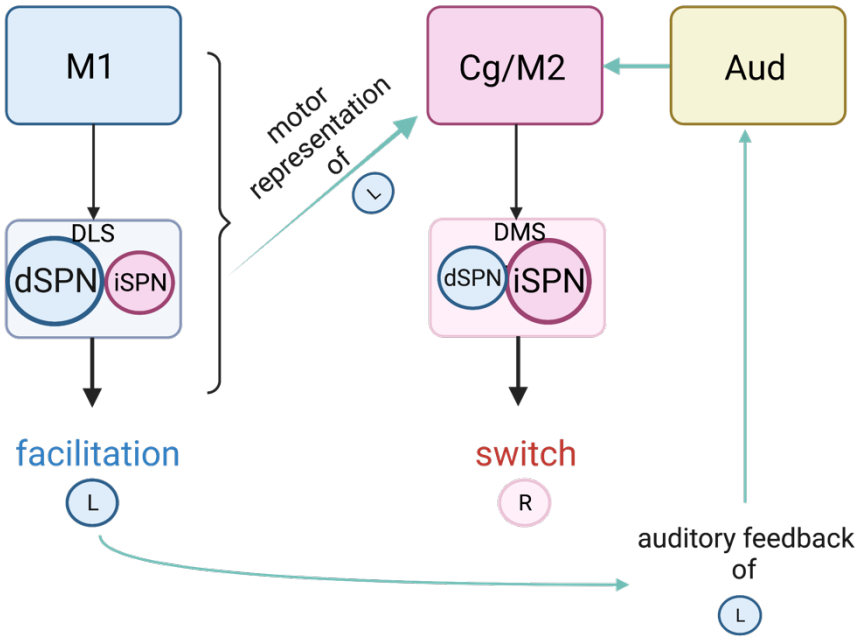

Figure 10. Model of parallel corticostriatal pathways in auditory feedback guided action sequencing

Summary diagram of the different roles of the M1–DLS pathway and the Cg/M2–DMS pathway in controlling auditory feedback-guided action sequence execution. The M1–DLS pathway signals the start of the action sequence and facilitates elemental actions through selectively activating the direct pathway in DLS. The representation of the motor command and auditory feedback of action are integrated in Cg/M2, which mediates between-subsequence at the proper timing through preferentially activating the indirect pathways in DMS.

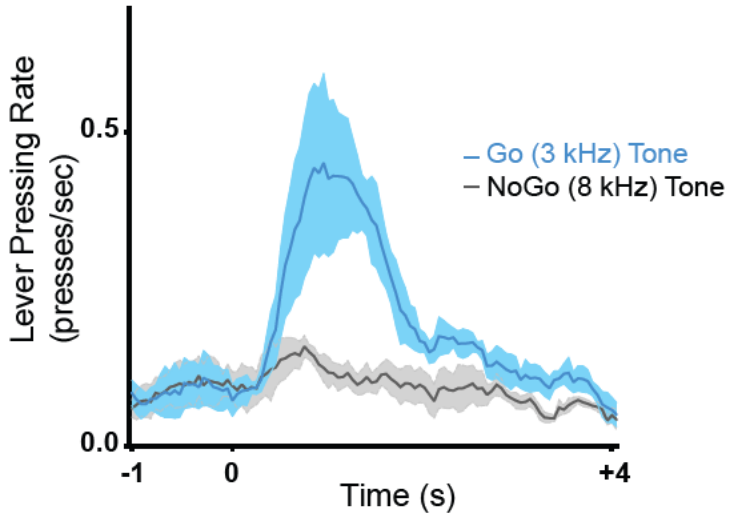

Figure S1. Mice can discriminate 3 kHz and 8kHz tones in Go/No Go task
After training in Go/No-Go task, mice (n=4) displayed high lever-pressing rate in response to the 3kHz Go tone and lever-pressing rate similar to the baseline in response to the 8kHz No-Go tone. Time zero was aligned at the onset of Go or No-Go tone (main effect of time: $F_{101,606}$ =6.64, p<0.0001; main effect of Go/No-Go tone: $F_{1,6}$=12.19, p=0.0130; time x tone interaction: $F_{101,606}$ =3.74, p<0.0001). Data were analyzed using repeated-measures two-way ANOVA. Error bars denote SEM.

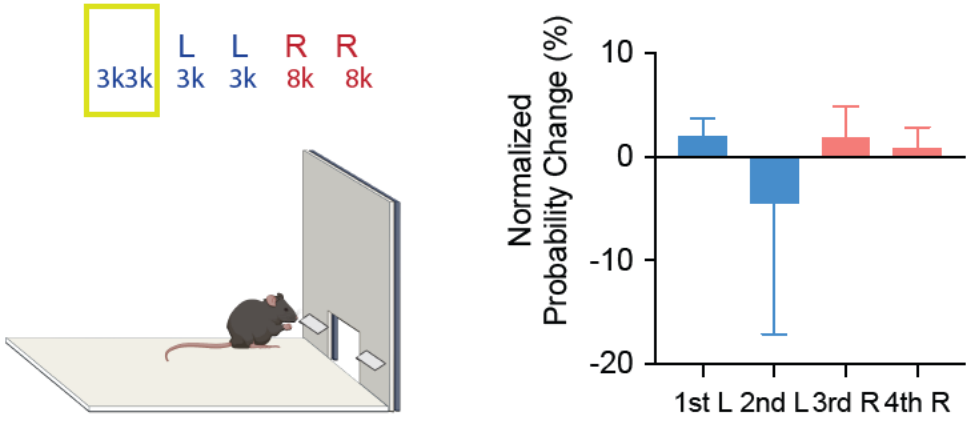

Figure S2. Auditory stimuli dissociated with action do not incur changes in action sequence execution

Two 3 kHz tones were delivered right before LLRR sequence initiation triggered by infrared beam break as mice approached the left lever (n=6). The bar graphs indicate normalized changes in probability for the four positions of the action sequence to be left press (1st L), be a left press (2nd L), a right press (3rd R), and a right press (4th R), respectively, following the second 3 kHz triggered by infrared beam break (1st L: t_5=1.616, p= 0.1669; 2nd L: t_5=0.4726, p= 0.6564; 3rd R: t_5=1.174, p= 0.2932; 4th R: t_5=0.4371, p= 0.6803). The data were analyzed with pair t-tests. Error bars denote SEM.

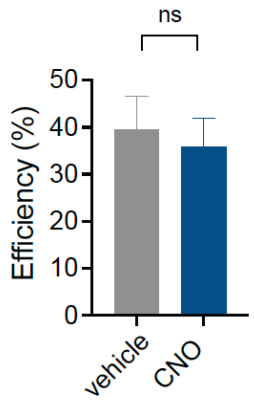

Figure S3. Chemogenetic silencing of the auditory cortex to the posterior striatum projections does not significantly alter auditory feedback-assisted sequence performance
AAV-hSyn-hMD4(Gi)-mCherry was injected into the auditory cortex and the posterior striatum was implanted with a cannula for drug delivery; these procedures were done bilaterally. Behavioral efficiency for trained mice injected with inhibitory Gi DREADDs on the day infused with CNO versus on the day infused with vehicle into the posterior striatum 30 minutes prior to test session of auditory feedback-assisted task (n=5, paired t-test, t4=2.535, p=0.0643).
Error bars denote SEM

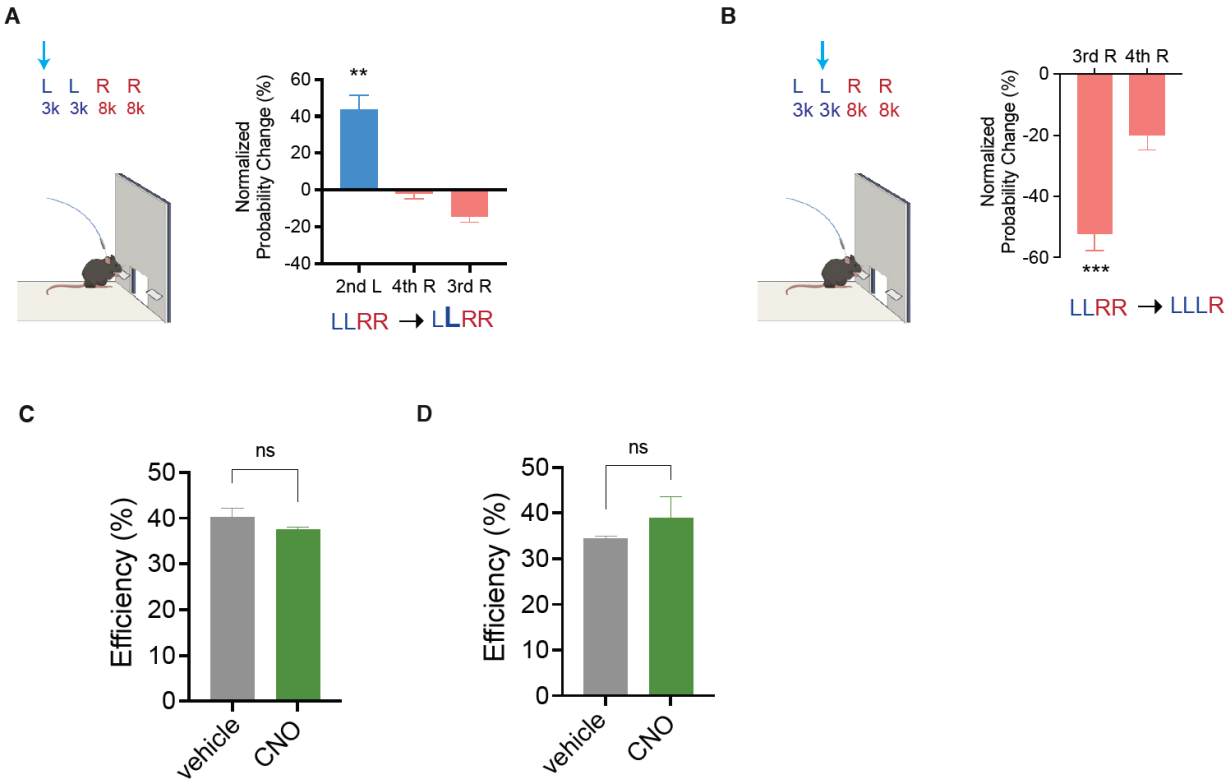

Figure S4. Optogenetic inhibition of OFC alters action sequence execution whereas chemogenetic silencing of the auditory cortex to OFC projections does not impair performance

(A and B) Optogenetic inhibition (by stimulating inhibitory interneurons in OFC) following the first (A) or the second left (B) press of the sequence when the trained Vgat Ai32 mice performed the auditory feedback-assisted task. 500-ms 473nm light was delivered triggered by the selected lever presses within the sequence, in randomly chosen probe trials. The bar graphs indicate normalized changes in probability for the succeeding elements to be a left press (2^{nd} L), a right press (3^{rd} R), and a right press (4^{th} R) subsequently, following optogenetic inhibition on the first left (A) or the second left press (B) (A: n=5, 2nd L: paired t-test, t_4=5.285, p=0.0062. B: n=5, 3rd R: paired t-test, t_4=8.794, p=0.0009).

(C and D) Chemogenetic inhibition of the auditory cortex–OFC terminals during auditory feedback-assisted task. AAV-hSyn hMD4(Gi)-mCherry or control AAV (which carries only fluorescent proteins) was injected into the auditory cortex and OFC was implanted with a cannula for drug delivery; the procedures were done bilaterally.

(C) Behavioral efficiency of trained mice injected with inhibitory Gi DREADDs on the day infused with CNO versus on the day infused with vehicle into OFC 30 minutes prior to the session (n=5, paired t-test, t4=1.432, p=0.2278).

(D) Behavioral efficiency of trained mice injected with control AAV on the day infused with CNO versus on the day infused with vehicle into OFC 30 minutes prior to the session (n=5, paired t-test, t4=0.9270, p=0.4223).

Error bars denote SEM.

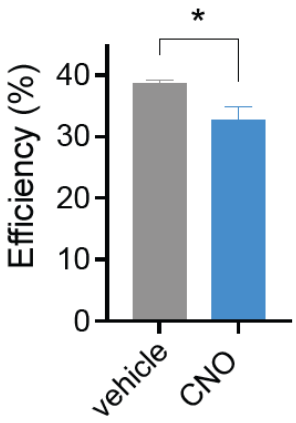

Figure S5. Chemogenetic silencing of M1 to Cg/M2 projection attenuates auditory feedback-assisted sequence performance

Chemogenetic inhibition of the M1–Cg/M2 terminals during auditory feedback-assisted task. AAV-hSyn hMD4(Gi)-mCherry was injected into M1 and Cg/M2 was implanted with a cannula for drug delivery; the procedures were done bilaterally. Behavioral efficiency of trained mice injected with inhibitory Gi DREADDs on the day infused with CNO and on the day infused with vehicle into M1, 30 minutes prior to the session of auditory feedback-assisted task (n=5, paired t-test, t_4=3.567, p=0.0234). Error bars denote SEM.

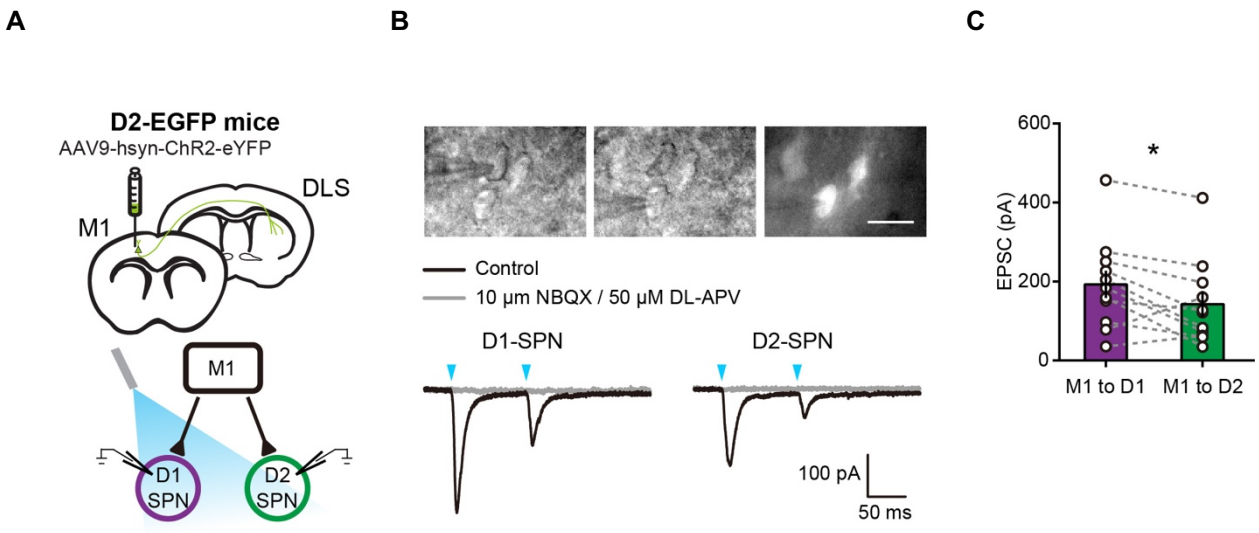

(Baibing Zhang, unpublished)

Figure S6. M1 cortical inputs differentially excite dSPNs vs. iSPNs in DLS
(A) Diagram of slice electrophysiological recording of dSPNs/iSPNs in DLS when activating M1 terminals. AAV9 hSyn-ChR2-eYFP was injected into M1 of D2-EGFP mice and recorded SPNs were all located in DLS.
(B) Example of optogenetic evoked EPSCs in a pair of neighboring dSPN and iSPN.
(C) Statistics of evoked EPSCs in pairs of dSPNs and iSPNs when activating M1 terminals (EPSCs of dSPNs: 192.5 ± 34.5 pA, EPSCs of iSPNs: 142.8 ± 32.89 pA, n= 11 pairs; paired t-test: p=0.029).

Chapter 5: Discussion and conclusion

Our everyday behavior is composed of diversified action sequences. Rapid integration of real-time sensory feedback generated by one's action enables rather swift, effortless execution of learned action sequences. To investigate how the sensory feedback and motor signals are integrated in the brain, we trained mice to learn a heterogeneous action sequence (LLRR) under the guidance of discriminative auditory feedback. This particular experimental design allows us to manipulate the auditory feedback on selected sequence positions and observe the change in online action selection. Transitioning from one type of action to another at an optimal moment is fundamental to human and animal behavior. Here we uncovered a circuit mechanism through which sensorimotor feedback is utilized to assist moment-to-moment action selection and guide behavioral switches. Our study reveals that the anterior cingulate cortex/secondary motor cortex (Cg/M2) region is accountable for integrating sensorimotor feedback signals and mediating subsequence switches in the motor program via its projection to the dorsomedial striatum (DMS).

In the current study, we provided artificial sensory feedback using auditory tones to denote different actions (L- or R-lever pressing). Previous studies have suggested that auditory stimuli are tightly coupled to temporal information of action (Burr, Banks, & Morrone, 2009; Cook et al., 2022; Kubovy, 1988; Repp & Penel, 2002) and thus an ideal feedback type for studying online action control in our task, as opposed to visual stimuli. Mice can readily discriminate a 3kHz from an 8kHz pure tone as shown in a two-category

auditory GO/NO-GO task (Fig. S1). Based on models of sensorimotor integration (Shadmehr & Krakauer, 2008; Wolpert, Ghahramani, & Jordan, 1995; Wolpert & Kawato, 1998), when motor commands are generated, our brains also make feedforward predictions about the sensory consequences. The actual sensory feedback will be compared with the predicted sensory feedback; a mismatch between these two can elicit rapid corrective signals to the motor controllers for updating motor commands. In the current study, we observed that manipulation of auditory feedback modulates online action selection and these effects art highly sequence state dependent. Omitting the expected auditory feedback on either the first or second position of the four-press sequence (the first subsequence) renders the animals to more likely repeat the same action and thus prevents subsequence switching, while introducing 'future auditory feedback' promotes switching. (Figures 2A–D). By contrast, perturbing the auditory feedback of the third position does not influence action selection. This can be explained by a default high probability of choosing R on the final position. These results suggest a dynamic weighting of auditory feedback relative to motor planning for action control based on sequence positions. Regarding our auditory feedback-assisted action sequence task, one might wonder whether it is purely perceptual learning such that mice merely learn the association between tones and reward, not the action sequence itself. If this is the case, one can expect that if the animals hear two 3 kHz (L) tones right before initiating the action sequence, they will choose to press the right lever to produce an 8kHz (R) tone. To test this possibility, we performed a control experiment, in which two consecutive 3kHz (L) tones were played when the animals approached the left lever, and this manipulation did not change their action selection. (Figures S2). This result suggests that mice did learn the action

sequence itself and performing this task requires integration of both sensory and motor information.

After auditory inputs reach cortical levels, the auditory cortex is the first hub that processes and relays the information. The primary auditory cortex encodes sound frequency tonotopically and has been shown to undergo tonotopic remapping following learning behaviorally relevant tones (Maor et al., 2019; Recanzone, Schreiner, & Merzenich, 1993; Rutkowski & Weinberger, 2005; Schreiner & Polley, 2014). Global inactivation of the auditory cortex during the task impairs execution of the learned sequence (Figure 3B), and optogenetically inhibition faithfully recapitulates the behavioral effects of omitting auditory feedback naturally (Figures 3C and D). Our antegrade tracing result reveals that the auditory cortex relays sensory inputs to multiple high-order association cortices, consistent with recent anatomical tracing data (Zingg et al., 2014). The auditory cortex also projects directly to the posterior tail of the dorsal striatum and this corticostriatal pathway has been shown to drive motor decisions in an auditory discrimination task (Xiong, Znamenskiy, & Zador, 2015). In the current study, however, chemogenetic inhibition of this pathway does not impair task performance (Figure S3). This result refutes the possibility that the posterior striatum is the principal site for integrating motor and sensory feedback representation. In addition, although the posterior striatum receives abundant auditory inputs, it lacks motor cortical inputs and has few iSPN (Gangarossa et al., 2013), which are critical for driving behavior switching in the task (Geddes, Li, & Jin, 2018). The posterior striatum is therefore less likely the integration region we searched for. In our screening with optogenetics, inhibition of orbitofrontal cortex (OFC) demonstrated comparable behavioral effects as Cg/M2. However, chemogenetic

inhibition of the auditory cortex–OFC does not affect sequence execution (Figure S4). This result indicates that OFC contributes to action control in our task in a manner independent of its auditory inputs. The mechanisms through which OFC regulates action sequence execution warrants further studies.

The ability to flexibly shift from one behavior to another is crucial for adapting to the constantly changing environment. Compelling evidence suggests that the anterior cingulate cortex plays an important role in adaptive switching between task or behavioral strategies through computing relevant parameters. (Economides, Guitart-Masip, Kurth-Nelson, & Dolan, 2014; Karlsson, Tervo, & Karpova, 2012; Kolling, Behrens, Mars, & Rushworth, 2012; Powell & Redish, 2016; Premereur, Janssen, & Vanduffel, 2018; Tervo et al., 2021) DMS and its inputs from the medial prefrontal cortex, including ACC, has also been implicated in flexible switching of behaviors (Bissonette & Roesch, 2017; Okada, Nishizawa, Setogawa, Hashimoto, & Kobayashi, 2018). The findings in the present study extend the current understanding by showing that Cg/M2 integrates moment-to-moment sensorimotor feedback to dictate behavioral switching at the subsequence level through the projection to DMS. The striatal indirect pathway has previously been shown to inhibit ongoing actions and mediates subsequence switch (Geddes et al., 2018). Slice electrophysiology revealed that Cg/M2 preferentially innervates the indirect pathway projection neurons (iSPN) (Figure 8), suggesting a possible mechanism that Cg/M2–DMS triggers subsequence switch through selectively activating the indirect pathway. In vivo electrophysiological recording of Cg/M2 further supports its role in behavioral switching by identifying a portion of switch-related neurons (Figures 7A and B), similar to the pattern previously found in iSPN (Geddes et al.,

2018). We also identified Cg/M2 neurons can encode unexpected auditory feedback. (Figures 7F and G). A wealth of evidence from studies in human, non-human primates and rodents strongly supports the role of the anterior cingulate cortex (ACC) in online performance monitoring and behavioral error detecting (Alexander & Brown, 2019; Carter et al., 1998; Eder & Dignath, 2019; Kiehl, Liddle, & Hopfinger, 2000; Rushworth & Behrens, 2008). EEG and fMRI studies report the presence of prediction error (PEs) signals in ACC (Debener et al., 2005; Holroyd et al., 2004; Miltner, Braun, & Coles, 1997) and SMA (human homolog of rodent M2) (Jahn, Nee, Alexander, & Brown, 2016). In vivo neuronal recordings further reveal that ACC neurons can represent both positive and negative PEs (Emeric et al., 2008; Ito, Stuphorn, Brown, & Schall, 2003; Kennerley, Behrens, & Wallis, 2011; reviewed in Shenhav, Botvinick, & Cohen, 2013). Our findings are consistent with recent models that suggest ACC computes a broad range of unpredicted events (Alexander & Brown, 2019), and further lend support to the proposed role of ACC in predictive coding, a critical component of sensorimotor integration. In addition, we also identified Cg/M2 neurons that faithfully respond to auditory tones (Figures 7D and E). Cg/M2 receives innervations from the auditory cortex and has been shown to displays neural responses to both behaviorally relevant and non-relevant auditory stimuli (Ebbesen et al., 2018; Fritz, David, Radtke-Schuller, Yin, & Shamma, 2010; Gallero-Salas et al., 2021; Khani et al., 2019; Rodgers & DeWeese, 2014). Yet there are no previously reported Cg/M2 neurons demonstrating such narrow widths, resembling that of the auditory cortical responses. This result suggests Cg/M2 might flexibly be entrained to represent auditory feedback, an essential factor needed for deciding when to switch. However, to confirm whether the observed neuronal responses are entrained by the task or default response, further studies are warranted.

It has been proposed that the dopamine system exerts a bimodal effect on the ACC network, which corresponds to the evaluation and execution phase of decision-making (reviewed in Assadi, Yucel, & Pantelis, 2009). This hypothesis is based on the previous observation that prefrontal activity can be modulated by the dopaminergic (DA) system (Seamans, Gorelova, Durstewitz, & Yang, 2001; Trantham-Davidson, Neely, Lavin, & Seamans, 2004; Lapish, Kroener, Durstewitz, Lavin, & Seamans, 2007). This model proposes that phasic, high concentrations of DA induce transient, predominantly D2 receptor activation, resulting in reduced net network inhibition. This change allows multiple inputs to present simultaneously in the prefrontal networks. By contrast, tonic, low concentrations of DA induce primarily D1 activation, resulting in increased net inhibition. At this long-lasting D1 state, only strong inputs have access to the network. The D2 state allows the concurrent multiple representations critical for the evaluation process, and then the D1 state stabilizes only the representation for the selected goal. Regarding this notion, it is possible that during action sequencing, the D2 state in Cg/M2 enables the integration of sensory feedback and motor representation, and the D1 state coincides with the execution of behavioral switching. To elucidate the mechanism underlying the transition between the "integration" and "switch" phase in Cg/M2, it will be worthwhile to investigate the dynamics of DA in Cg/M2 and its influence on different neuronal populations.

In the present study, we identified two parallel corticostriatal pathways working coordinately during performing a heterogeneous action sequence: the M1–DLS pathway facilitates ongoing actions, while the Cg/M2–DMS pathway guides behavioral switching. Our findings are consistent with past studies showing that DLS is required for the execution of

sequences comprising the same type of action (Yin, 2010), and DLS striatal neurons demonstrate start-related activity and continuous activity during sequence execution (Jin & Costa, 2010; Jin, Tecuapetla, & Costa, 2014; Jog, Kubota, Connolly, Hillegaart, & Graybiel, 1999). M1 and its DLS projections have been shown to be critical for motor skills and action sequence acquisition (Lemke, Ramanathan, Guo, Won, & Ganguly, 2019; Santos, Oliveira, Jin, & Costa, 2015), and M1 encodes individual elements of the sequence (Yokoi & Diedrichsen, 2019). Moreover, our findings also extend the current understanding of corticostriatal circuitry. The associative corticostriatal circuits (PFC–DMS) are implicated in goal-directed behaviors and sensorimotor corticostriatal circuits (sensorimotor cortices–DLS) are implicated in habitual behaviors. A prevailing view of skill learning is that the control of action is shifted from the prefrontal-DMS pathways to the sensorimotor cortices–DLS pathways (Floyer-Lea & Matthews, 2005; Lehericy et al., 2005; Miyachi, Hikosaka, & Lu, 2002). Here we showed that to execute action sequences that require behavioral switching, both pathways are engaged and work coordinately. A recent study also reported the involvement of both pathways during skill performance (Kupferschmidt, Juczewski, Cui, Johnson, & Lovinger, 2017). In our proposed model, Cg/M2 integrates actual sensory feedback and motor representation as a predictive signal of sensory feedback. Chemogenetic inhibition of M1 terminals in Cg/M2 interfered with the execution of action sequence (Figure S5). This result suggests Cg/M2 may receive the representation of motor signal directly from M1. However, it does not rule out the possibility that other sources also transmit the motor representation from M1-DLS pathways to Cg/M2. The cerebellum has been proposed to contain feedforward models and generate the feedforward predictive signal for sensory outcomes (Blakemore, Frith, & Wolpert, 2001; Wolpert, Miall, & Kawato, 1998). The

cerebellum and the anterior cingulate cortex (ACC) similarly display decreased activity associated with self-generated tactile stimulation compared to when it is generated externally (Blakemore, Wolpert, & Frith, 1998). Anatomically, M1 sends projections to pontine nucleus which generates mossy fibers to the cerebellar cortex, and the cerebellar nucleus sends projections to the thalamus which can further connect Cg/M2 (Munoz-Castaneda et al., 2021). What role the cerebellum plays in sensorimotor integration that supports action sequencing requires further studies.

Implications

The present study identified the role of Cg/M2 in sensorimotor integration and action sequencing, and our findings potentially provide a comprehensive perspective of how Cg/M2 dysfunction contributes to both psychotic symptoms and cognitive deficits in schizophrenia. Failing to properly integrate sensory feedback and motor representation is thought to underlie the pathophysiology of agency-related psychotic symptoms such as auditory hallucination (AH), thought insertion or delusion of being controlled in patients with schizophrenia (Feinberg, 1978). Experimental data on various sensorimotor domains, including speech, touch and oculomotor movement, further support the hypothesized integration failure in SCZ patients. (Ford, Gray, Faustman, Roach, & Mathalon, 2007; Ford et al., 2001; Shergill, Samson, Bays, Frith, & Wolpert, 2005; Thakkar & Rolfs, 2019). Past studies implicated ACC dysfunction in schizophrenia (Adams & David, 2007). The activity of ACC is associated with processing inner speech (Medalla & Barbas, 2014; Perrone-Bertolotti, Rapin, Lachaux, Baciu, & Loevenbruck, 2014; Simons et al., 2010). Patients with AH showed impaired connectivity

between ACC and speech perception region left superior temporal lobe when evaluating their own speech (Mechelli et al., 2007). In a conditioning induced hallucination paradigm, ACC was shown to be engaged during conditioned AH. During correct rejections, patients with AH displayed much lower activity in ACC compared to normal subjects (Powers, Mathys, & Corlett, 2017). In addition, patients with schizophrenia also have deficits in prediction error (PE) processing (Waltz et al., 2018; Yaple, Tolomeo, & Yu, 2021), and mid-frontal stimulation improved PE processing in SCZ patients (Reinhart, Zhu, Park, & Woodman, 2015). Findings from an early study hinted that ACC could be involved in corollary discharge mechanisms (Blakemore et al., 1998) and the present work supports this possibility. Our findings clearly support that ACC dysfunction could cause psychotic symptoms due to aberrant sensorimotor integration. We further reveal the Cg/M2–DMS pathways specifically controls behavioral switching during action sequencing. SCZ patients are well-known to demonstrate set-shifting deficits (Ceaser et al., 2008; Jazbec et al., 2007; Leeson et al., 2009; Pantelis et al., 1999) that they have profound difficulties in inhibiting their responses to the current dimension and shifting to a different dimension. Studies also reported reduced functional and structural connectivity between the prefrontal cortex and striatum in SCZ patients (Fornito et al., 2013; Levitt et al., 2017). Our data further suggest that dysfunction of Cg/M2 and its DMS projection sabotages the organization of action sequences, which might also lead to disturbance in hierarchical programming of thought process and result in formal thought disorders in SCZ patients.

The current treatment of schizophrenia centers around dopaminergic (DA) D2 receptor antagonism (Kambeitz, Abi-Dargham, Kapur, & Howes, 2014). Several studies suggest that

antipsychotic action works primarily through extrastriatal D2 receptors (Joyce & Meador-Woodruff, 1997; Lidow, Williams, & Goldman-Rakic, 1998; Winterer & Weinberger, 2004; reviewed in Takahashi, Higuchi, & Suhara, 2006) and recent evidence highlights the role of cortical dopaminergic D2 receptors in SCZ pathophysiology (Takahashi, Higuchi, & Suhara, 2006). Particularly, decreased D2 receptor binding in ACC was noted in SCZ patients (Suhara et al., 2002; Yasuno et al., 2005) and there was a negative correlation between D2 binding and positive symptoms (Suhara et al., 2002). Postmortem studies also revelated dysregulated DA innervations in ACC, particularly in layer II (Benes, 2000) which receives intracortical information flow. As previously discussed in this chapter, D2 activation in ACC might facilitate presentation of multiple sensorimotor information. Disrupted D2 binding in ACC could thus interfere with sensorimotor integration and further impair mental action sequencing, leading to psychotic symptoms and cognitive deficits in SCZ patients.

Conclusion and future directions

In the present study, we successfully established a mouse model to study auditory-motor integration in action sequencing. Our data indicate that Cg/M2 integrates sensory feedback and motor signals for making the crucial decision of subsequence switch, which is mediated by Cg/M2–DMS projection. We further demonstrate that the M1–DLS pathway and the Cg/M2–DMS pathway coordinately in action sequencing. The M1–Cg/M2 projection serves as one route through which the motor representation is transmitted. Overall, our findings reveal an essential neural mechanism of sensorimotor feedback in action sequencing

and provide important insights into understanding the pathophysiology of schizophrenia. Some future directions for studying include (1) the role of the cerebellum– a region implicated in corollary discharge signaling, (2) the role of dopamine signaling in Cg/M2 for sensorimotor integration, and (3) cellular mechanisms and local circuits within Cg/M2 for computing and decision making.

Part of chapter 5 is currently being prepared for submission for publication of the material. (Huang, Hsiang-Hsuan; Yan, Xunyi; Zhang, Baibing; Jin, Xin.) The dissertation author was the primary researcher and author of this material.

References

Adams, R., & David, A. S. (2007). Patterns of anterior cingulate activation in schizophrenia: a selective review. *Neuropsychiatr Dis Treat, 3*(1), 87-101. doi:10.2147/nedt.2007.3.1.87

Alexander, W. H., & Brown, J. W. (2019). The Role of the Anterior Cingulate Cortex in Prediction Error and Signaling Surprise. *Top Cogn Sci, 11*(1), 119-135. doi:10.1111/tops.12307

Assadi, S. M., Yucel, M., & Pantelis, C. (2009). Dopamine modulates neural networks involved in effort-based decision-making. *Neurosci Biobehav Rev, 33*(3), 383-393. doi:10.1016/j.neubiorev.2008.10.010

Benes, F. M. (2000). Emerging principles of altered neural circuitry in schizophrenia. *Brain Res Brain Res Rev, 31*(2-3), 251-269. doi:10.1016/s0165-0173(99)00041-7

Bissonette, G. B., & Roesch, M. R. (2017). Neurophysiology of Rule Switching in the Corticostriatal Circuit. *Neuroscience, 345*, 64-76. doi:10.1016/j.neuroscience.2016.01.062

Blakemore, S. J., Frith, C. D., & Wolpert, D. M. (2001). The cerebellum is involved in predicting the sensory consequences of action. *Neuroreport, 12*(9), 1879-1884. doi:Doi 10.1097/00001756-200107030-00023

Blakemore, S. J., Wolpert, D. M., & Frith, C. D. (1998). Central cancellation of self-produced tickle sensation. *Nature Neuroscience, 1*(7), 635-640. doi:Doi 10.1038/2870

Burr, D., Banks, M. S., & Morrone, M. C. (2009). Auditory dominance over vision in the perception of interval duration. *Exp Brain Res, 198*(1), 49-57. doi:10.1007/s00221-009-1933-z

Carter, C. S., Braver, T. S., Barch, D. M., Botvinick, M. M., Noll, D., & Cohen, J. D. (1998). Anterior cingulate cortex, error detection, and the online monitoring of performance. *Science, 280*(5364), 747-749. doi:10.1126/science.280.5364.747

Ceaser, A. E., Goldberg, T. E., Egan, M. F., McMahon, R. P., Weinberger, D. R., & Gold, J. M. (2008). Set-shifting ability and schizophrenia: a marker of clinical illness or an intermediate phenotype? *Biol Psychiatry, 64*(9), 782-788. doi:10.1016/j.biopsych.2008.05.009

Cook, J. R., Li, H., Nguyen, B., Huang, H. H., Mahdavian, P., Kirchgessner, M. A., . . . Jin, X. (2022). Secondary auditory cortex mediates a sensorimotor mechanism for action timing. *Nat Neurosci, 25*(3), 330-344. doi:10.1038/s41593-022-01025-5

Debener, S., Ullsperger, M., Siegel, M., Fiehler, K., von Cramon, D. Y., & Engel, A. K. (2005). Trial-by-trial coupling of concurrent electroencephalogram and functional

magnetic resonance imaging identifies the dynamics of performance monitoring. *J Neurosci, 25*(50), 11730-11737. doi:10.1523/JNEUROSCI.3286-05.2005

Ebbesen, C. L., Insanally, M. N., Kopec, C. D., Murakami, M., Saiki, A., & Erlich, J. C. (2018). More than Just a "Motor": Recent Surprises from the Frontal Cortex. *J Neurosci, 38*(44), 9402-9413. doi:10.1523/JNEUROSCI.1671-18.2018

Economides, M., Guitart-Masip, M., Kurth-Nelson, Z., & Dolan, R. J. (2014). Anterior Cingulate Cortex Instigates Adaptive Switches in Choice by Integrating Immediate and Delayed Components of Value in Ventromedial Prefrontal Cortex. *Journal of Neuroscience, 34*(9), 3340-3349. doi:10.1523/Jneurosci.4313-13.2014

Eder, A. B., & Dignath, D. (2019). Expected Value of Control and the Motivational Control of Habitual Action. *Front Psychol, 10*, 1812. doi:10.3389/fpsyg.2019.01812

Emeric, E. E., Brown, J. W., Leslie, M., Pouget, P., Stuphorn, V., & Schall, J. D. (2008). Performance monitoring local field potentials in the medial frontal cortex of primates: anterior cingulate cortex. *J Neurophysiol, 99*(2), 759-772. doi:10.1152/jn.00896.2006

Feinberg, I. (1978). Efference copy and corollary discharge: implications for thinking and its disorders. *Schizophr Bull, 4*(4), 636-640. doi:10.1093/schbul/4.4.636

Floyer-Lea, A., & Matthews, P. M. (2005). Distinguishable brain activation networks for short- and long-term motor skill learning. *J Neurophysiol, 94*(1), 512-518. doi:10.1152/jn.00717.2004

Ford, J. M., Gray, M., Faustman, W. O., Roach, B. J., & Mathalon, D. H. (2007). Dissecting corollary discharge dysfunction in schizophrenia. *Psychophysiology, 44*(4), 522-529. doi:10.1111/j.1469-8986.2007.00533.x

Ford, J. M., Mathalon, D. H., Kalba, S., Whitfield, S., Faustman, W. O., & Roth, W. T. (2001). Cortical responsiveness during talking and listening in schizophrenia: an event-related brain potential study. *Biol Psychiatry, 50*(7), 540-549. doi:10.1016/s0006-3223(01)01166-0

Fornito, A., Harrison, B. J., Goodby, E., Dean, A., Ooi, C., Nathan, P. J., . . . Bullmore, E. T. (2013). Functional Dysconnectivity of Corticostriatal Circuitry as a Risk Phenotype for Psychosis. *Jama Psychiatry, 70*(11), 1143-1151. doi:10.1001/jamapsychiatry.2013.1976

Fritz, J. B., David, S. V., Radtke-Schuller, S., Yin, P., & Shamma, S. A. (2010). Adaptive, behaviorally gated, persistent encoding of task-relevant auditory information in ferret frontal cortex. *Nat Neurosci, 13*(8), 1011-1019. doi:10.1038/nn.2598

Gallero-Salas, Y., Han, S., Sych, Y., Voigt, F. F., Laurenczy, B., Gilad, A., & Helmchen, F. (2021). Sensory and Behavioral Components of Neocortical Signal Flow in

Discrimination Tasks with Short-Term Memory. *Neuron, 109*(1), 135-148 e136. doi:10.1016/j.neuron.2020.10.017

Gangarossa, G., Espallergues, J., Mailly, P., De Bundel, D., de Kerchove d'Exaerde, A., Herve, D., . . . Krieger, P. (2013). Spatial distribution of D1R- and D2R-expressing medium-sized spiny neurons differs along the rostro-caudal axis of the mouse dorsal striatum. *Front Neural Circuits, 7*, 124. doi:10.3389/fncir.2013.00124

Geddes, C. E., Li, H., & Jin, X. (2018). Optogenetic Editing Reveals the Hierarchical Organization of Learned Action Sequences. *Cell, 174*(1), 32-43 e15. doi:10.1016/j.cell.2018.06.012

Holroyd, C. B., Nieuwenhuis, S., Yeung, N., Nystrom, L., Mars, R. B., Coles, M. G., & Cohen, J. D. (2004). Dorsal anterior cingulate cortex shows fMRI response to internal and external error signals. *Nat Neurosci, 7*(5), 497-498. doi:10.1038/nn1238

Ito, S., Stuphorn, V., Brown, J. W., & Schall, J. D. (2003). Performance monitoring by the anterior cingulate cortex during saccade countermanding. *Science, 302*(5642), 120-122. doi:10.1126/science.1087847

Jahn, A., Nee, D. E., Alexander, W. H., & Brown, J. W. (2016). Distinct Regions within Medial Prefrontal Cortex Process Pain and Cognition. *J Neurosci, 36*(49), 12385-12392. doi:10.1523/JNEUROSCI.2180-16.2016

Jazbec, S., Pantelis, C., Robbins, T., Weickert, T., Weinberger, D. R., & Goldberg, T. E. (2007). Intra-dimensional/extra-dimensional set-shifting performance in schizophrenia: impact of distractors. *Schizophrenia Research, 89*(1-3), 339-349. doi:10.1016/j.schres.2006.08.014

Jin, X., & Costa, R. M. (2010). Start/stop signals emerge in nigrostriatal circuits during sequence learning. *Nature, 466*(7305), 457-462. doi:10.1038/nature09263

Jin, X., Tecuapetla, F., & Costa, R. M. (2014). Basal ganglia subcircuits distinctively encode the parsing and concatenation of action sequences. *Nat Neurosci, 17*(3), 423-430. doi:10.1038/nn.3632

Jog, M. S., Kubota, Y., Connolly, C. I., Hillegaart, V., & Graybiel, A. M. (1999). Building neural representations of habits. *Science, 286*(5445), 1745-1749. doi:DOI 10.1126/science.286.5445.1745

Joyce, J. N., & Meador-Woodruff, J. H. (1997). Linking the family of D2 receptors to neuronal circuits in human brain: insights into schizophrenia. *Neuropsychopharmacology, 16*(6), 375-384. doi:10.1016/S0893-133X(96)00276-X

Kambeitz, J., Abi-Dargham, A., Kapur, S., & Howes, O. D. (2014). Alterations in cortical and extrastriatal subcortical dopamine function in schizophrenia: systematic review and

meta-analysis of imaging studies. *Br J Psychiatry, 204*(6), 420-429. doi:10.1192/bjp.bp.113.132308

Karlsson, M. P., Tervo, D. G. R., & Karpova, A. Y. (2012). Network Resets in Medial Prefrontal Cortex Mark the Onset of Behavioral Uncertainty. *Science, 338*(6103), 135-139. doi:10.1126/science.1226518

Kennerley, S. W., Behrens, T. E., & Wallis, J. D. (2011). Double dissociation of value computations in orbitofrontal and anterior cingulate neurons. *Nat Neurosci, 14*(12), 1581-1589. doi:10.1038/nn.2961

Khani, A., Lanz, F., Loquet, G., Schaller, K., Michel, C., & Quairiaux, C. (2019). Large-Scale Networks for Auditory Sensory Gating in the Awake Mouse. *eNeuro, 6*(5). doi:10.1523/ENEURO.0207-19.2019

Kiehl, K. A., Liddle, P. F., & Hopfinger, J. B. (2000). Error processing and the rostral anterior cingulate: an event-related fMRI study. *Psychophysiology, 37*(2), 216-223. Retrieved from https://www.ncbi.nlm.nih.gov/pubmed/10731771

Kolling, N., Behrens, T. E. J., Mars, R. B., & Rushworth, M. F. S. (2012). Neural Mechanisms of Foraging. *Science, 336*(6077), 95-98. doi:10.1126/science.1216930

Kubovy, M. (1988). Should We Resist the Seductiveness of the Space-Time, Vision-Audition Analogy. *Journal of Experimental Psychology-Human Perception and Performance, 14*(2), 318-320. doi:Doi 10.1037/0096-1523.14.2.318

Kupferschmidt, D. A., Juczewski, K., Cui, G., Johnson, K. A., & Lovinger, D. M. (2017). Parallel, but Dissociable, Processing in Discrete Corticostriatal Inputs Encodes Skill Learning. *Neuron, 96*(2), 476-489 e475. doi:10.1016/j.neuron.2017.09.040

Lapish, C. C., Kroener, S., Durstewitz, D., Lavin, A., & Seamans, J. K. (2007). The ability of the mesocortical dopamine system to operate in distinct temporal modes. *Psychopharmacology (Berl), 191*(3), 609-625. doi:10.1007/s00213-006-0527-8

Leeson, V. C., Robbins, T. W., Matheson, E., Hutton, S. B., Ron, M. A., Barnes, T. R., & Joyce, E. M. (2009). Discrimination learning, reversal, and set-shifting in first-episode schizophrenia: stability over six years and specific associations with medication type and disorganization syndrome. *Biol Psychiatry, 66*(6), 586-593. doi:10.1016/j.biopsych.2009.05.016

Lehericy, S., Benali, H., Van de Moortele, P. F., Pelegrini-Issac, M., Waechter, T., Ugurbil, K., & Doyon, J. (2005). Distinct basal ganglia territories are engaged in early and advanced motor sequence learning. *Proc Natl Acad Sci U S A, 102*(35), 12566-12571. doi:10.1073/pnas.0502762102

Lemke, S. M., Ramanathan, D. S., Guo, L., Won, S. J., & Ganguly, K. (2019). Emergent modular neural control drives coordinated motor actions. *Nat Neurosci, 22*(7), 1122-1131. doi:10.1038/s41593-019-0407-2

Levitt, J. J., Nestor, P. G., Levin, L., Pelavin, P., Lin, P., Kubicki, M., . . . Rathi, Y. (2017). Reduced Structural Connectivity in Frontostriatal White Matter Tracts in the Associative Loop in Schizophrenia. *American Journal of Psychiatry, 174*(11), 1102-1111. doi:10.1176/appi.ajp.2017.16091046

Lidow, M. S., Williams, G. V., & Goldman-Rakic, P. S. (1998). The cerebral cortex: a case for a common site of action of antipsychotics. *Trends Pharmacol Sci, 19*(4), 136-140. doi:10.1016/s0165-6147(98)01186-9

Maor, I., Shwartz-Ziv, R., Feigin, L., Elyada, Y., Sompolinsky, H., & Mizrahi, A. (2019). Neural Correlates of Learning Pure Tones or Natural Sounds in the Auditory Cortex. *Front Neural Circuits, 13*, 82. doi:10.3389/fncir.2019.00082

Mechelli, A., Allen, P., Amaro, E., Jr., Fu, C. H., Williams, S. C., Brammer, M. J., . . . McGuire, P. K. (2007). Misattribution of speech and impaired connectivity in patients with auditory verbal hallucinations. *Hum Brain Mapp, 28*(11), 1213-1222. doi:10.1002/hbm.20341

Medalla, M., & Barbas, H. (2014). Specialized prefrontal "auditory fields": organization of primate prefrontal-temporal pathways. *Frontiers in Neuroscience, 8*. doi:ARTN 77 10.3389/fnins.2014.00077

Miltner, W. H., Braun, C. H., & Coles, M. G. (1997). Event-related brain potentials following incorrect feedback in a time-estimation task: evidence for a "generic" neural system for error detection. *J Cogn Neurosci, 9*(6), 788-798. doi:10.1162/jocn.1997.9.6.788

Miyachi, S., Hikosaka, O., & Lu, X. (2002). Differential activation of monkey striatal neurons in the early and late stages of procedural learning. *Exp Brain Res, 146*(1), 122-126. doi:10.1007/s00221-002-1213-7

Munoz-Castaneda, R., Zingg, B., Matho, K. S., Chen, X., Wang, Q., Foster, N. N., . . . Dong, H. W. (2021). Cellular anatomy of the mouse primary motor cortex. *Nature, 598*(7879), 159-166. doi:10.1038/s41586-021-03970-w

Okada, K., Nishizawa, K., Setogawa, S., Hashimoto, K., & Kobayashi, K. (2018). Task-dependent function of striatal cholinergic interneurons in behavioural flexibility. *Eur J Neurosci, 47*(10), 1174-1183. doi:10.1111/ejn.13768

Pantelis, C., Barber, F. Z., Barnes, T. R., Nelson, H. E., Owen, A. M., & Robbins, T. W. (1999). Comparison of set-shifting ability in patients with chronic schizophrenia and frontal lobe damage. *Schizophrenia Research, 37*(3), 251-270. doi:10.1016/s0920-9964(98)00156-x

Perrone-Bertolotti, M., Rapin, L., Lachaux, J. P., Baciu, M., & Loevenbruck, H. (2014). What is that little voice inside my head? Inner speech phenomenology, its role in cognitive performance, and its relation to self-monitoring. *Behavioural Brain Research, 261*, 220-239. doi:10.1016/j.bbr.2013.12.034

Powell, N. J., & Redish, A. D. (2016). Representational changes of latent strategies in rat medial prefrontal cortex precede changes in behaviour. *Nat Commun, 7*, 12830. doi:10.1038/ncomms12830

Powers, A. R., Mathys, C., & Corlett, P. R. (2017). Pavlovian conditioning-induced hallucinations result from overweighting of perceptual priors. *Science, 357*(6351), 596-600. doi:10.1126/science.aan3458

Premereur, E., Janssen, P., & Vanduffel, W. (2018). Functional MRI in Macaque Monkeys during Task Switching. *Journal of Neuroscience, 38*(50), 10619-10630. doi:10.1523/Jneurosci.1539-18.2018

Recanzone, G. H., Schreiner, C. E., & Merzenich, M. M. (1993). Plasticity in the frequency representation of primary auditory cortex following discrimination training in adult owl monkeys. *J Neurosci, 13*(1), 87-103. Retrieved from https://www.ncbi.nlm.nih.gov/pubmed/8423485

Reinhart, R. M., Zhu, J., Park, S., & Woodman, G. F. (2015). Medial-Frontal Stimulation Enhances Learning in Schizophrenia by Restoring Prediction Error Signaling. *J Neurosci, 35*(35), 12232-12240. doi:10.1523/JNEUROSCI.1717-15.2015

Repp, B. H., & Penel, A. (2002). Auditory dominance in temporal processing: new evidence from synchronization with simultaneous visual and auditory sequences. *J Exp Psychol Hum Percept Perform, 28*(5), 1085-1099. Retrieved from https://www.ncbi.nlm.nih.gov/pubmed/12421057

Rodgers, C. C., & DeWeese, M. R. (2014). Neural correlates of task switching in prefrontal cortex and primary auditory cortex in a novel stimulus selection task for rodents. *Neuron, 82*(5), 1157-1170. doi:10.1016/j.neuron.2014.04.031

Rushworth, M. F., & Behrens, T. E. (2008). Choice, uncertainty and value in prefrontal and cingulate cortex. *Nat Neurosci, 11*(4), 389-397. doi:10.1038/nn2066

Rutkowski, R. G., & Weinberger, N. M. (2005). Encoding of learned importance of sound by magnitude of representational area in primary auditory cortex. *Proc Natl Acad Sci U S A, 102*(38), 13664-13669. doi:10.1073/pnas.0506838102

Santos, F. J., Oliveira, R. F., Jin, X., & Costa, R. M. (2015). Corticostriatal dynamics encode the refinement of specific behavioral variability during skill learning. *Elife, 4*, e09423. doi:10.7554/eLife.09423

Schreiner, C. E., & Polley, D. B. (2014). Auditory map plasticity: diversity in causes and consequences. *Curr Opin Neurobiol, 24*(1), 143-156. doi:10.1016/j.conb.2013.11.009

Seamans, J. K., Gorelova, N., Durstewitz, D., & Yang, C. R. (2001). Bidirectional dopamine modulation of GABAergic inhibition in prefrontal cortical pyramidal neurons. *J Neurosci, 21*(10), 3628-3638. Retrieved from https://www.ncbi.nlm.nih.gov/pubmed/11331392

Shadmehr, R., & Krakauer, J. W. (2008). A computational neuroanatomy for motor control. *Exp Brain Res, 185*(3), 359-381. doi:10.1007/s00221-008-1280-5

Shergill, S. S., Samson, G., Bays, P. M., Frith, C. D., & Wolpert, D. M. (2005). Evidence for sensory prediction deficits in schizophrenia. *Am J Psychiatry, 162*(12), 2384-2386. doi:10.1176/appi.ajp.162.12.2384

Shenhav, A., Botvinick, M. M., & Cohen, J. D. (2013). The expected value of control: an integrative theory of anterior cingulate cortex function. *Neuron, 79*(2), 217-240. doi:10.1016/j.neuron.2013.07.007

Simons, C. J., Tracy, D. K., Sanghera, K. K., O'Daly, O., Gilleen, J., Dominguez, M. D., . . . Shergill, S. S. (2010). Functional magnetic resonance imaging of inner speech in schizophrenia. *Biol Psychiatry, 67*(3), 232-237. doi:10.1016/j.biopsych.2009.09.007

Suhara, T., Okubo, Y., Yasuno, F., Sudo, Y., Inoue, M., Ichimiya, T., . . . Farde, L. (2002). Decreased dopamine D2 receptor binding in the anterior cingulate cortex in schizophrenia. *Arch Gen Psychiatry, 59*(1), 25-30. doi:10.1001/archpsyc.59.1.25

Takahashi, H., Higuchi, M., & Suhara, T. (2006). The role of extrastriatal dopamine D2 receptors in schizophrenia. *Biol Psychiatry, 59*(10), 919-928. doi:10.1016/j.biopsych.2006.01.022

Tervo, D. G. R., Kuleshova, E., Manakov, M., Proskurin, M., Karlsson, M., Lustig, A., . . . Karpova, A. Y. (2021). The anterior cingulate cortex directs exploration of alternative strategies. *Neuron, 109*(11), 1876-1887 e1876. doi:10.1016/j.neuron.2021.03.028

Thakkar, K. N., & Rolfs, M. (2019). Disrupted Corollary Discharge in Schizophrenia: Evidence From the Oculomotor System. *Biol Psychiatry Cogn Neurosci Neuroimaging, 4*(9), 773-781. doi:10.1016/j.bpsc.2019.03.009

Trantham-Davidson, H., Neely, L. C., Lavin, A., & Seamans, J. K. (2004). Mechanisms underlying differential D1 versus D2 dopamine receptor regulation of inhibition in prefrontal cortex. *J Neurosci, 24*(47), 10652-10659. doi:10.1523/JNEUROSCI.3179-04.2004

Waltz, J. A., Xu, Z. Y., Brown, E. C., Ruiz, R. R., Frank, M. J., & Gold, J. M. (2018). Motivational Deficits in Schizophrenia Are Associated With Reduced Differentiation

Between Gain and Loss-Avoidance Feedback in the Striatum. *Biological Psychiatry-Cognitive Neuroscience and Neuroimaging, 3*(3), 239-247. doi:10.1016/j.bpsc.2017.07.008

Winterer, G., & Weinberger, D. R. (2004). Genes, dopamine and cortical signal-to-noise ratio in schizophrenia. *Trends Neurosci, 27*(11), 683-690. doi:10.1016/j.tins.2004.08.002

Wolpert, D. M., Ghahramani, Z., & Jordan, M. I. (1995). An internal model for sensorimotor integration. *Science, 269*(5232), 1880-1882. doi:10.1126/science.7569931

Wolpert, D. M., & Kawato, M. (1998). Multiple paired forward and inverse models for motor control. *Neural Netw, 11*(7-8), 1317-1329. doi:10.1016/s0893-6080(98)00066-5

Wolpert, D. M., Miall, R. C., & Kawato, M. (1998). Internal models in the cerebellum. *Trends in Cognitive Sciences, 2*(9), 338-347. doi:Doi 10.1016/S1364-6613(98)01221-2

Xiong, Q., Znamenskiy, P., & Zador, A. M. (2015). Selective corticostriatal plasticity during acquisition of an auditory discrimination task. *Nature, 521*(7552), 348-351. doi:10.1038/nature14225

Yaple, Z. A., Tolomeo, S., & Yu, R. (2021). Abnormal prediction error processing in schizophrenia and depression. *Hum Brain Mapp, 42*(11), 3547-3560. doi:10.1002/hbm.25453

Yasuno, F., Suhara, T., Okubo, Y., Ichimiya, T., Takano, A., Sudo, Y., & Inoue, M. (2005). Abnormal effective connectivity of dopamine D2 receptor binding in schizophrenia. *Psychiatry Res, 138*(3), 197-207. doi:10.1016/j.pscychresns.2004.04.005

Yin, H. H. (2010). The Sensorimotor Striatum Is Necessary for Serial Order Learning. *Journal of Neuroscience, 30*(44), 14719-14723. doi:10.1523/Jneurosci.3989-10.2010

Yokoi, A., & Diedrichsen, J. (2019). Neural Organization of Hierarchical Motor Sequence Representations in the Human Neocortex. *Neuron, 103*(6), 1178-1190 e1177. doi:10.1016/j.neuron.2019.06.017

Zingg, B., Hintiryan, H., Gou, L., Song, M. Y., Bay, M., Bienkowski, M. S., . . . Dong, H. W. (2014). Neural Networks of the Mouse Neocortex. *Cell, 156*(5), 1096-1111. doi:10.1016/j.cell.2014.02.023

Appendix: Methods

Subjects

All experimental procedures were reviewed and approved by the Institutional Animal Care and Use Committee at the Salk Institute and followed the National Institute of Health's Guide for the Care and Use of Laboratory Animals. Experiments were performed with both male and female mice at least two months old, which were maintained on a 12-hour light/dark cycle with regular chow and water ad libitum. Wild-type mice with a C57BL/6 background (Envigo/Harlan) were used for most experiments if not else mentioned. Vgat-Ai32 mice were obtained by crossing Vgat-Cre (Jackson Laboratory: 028862) with Ai32 mice (Jackson Laboratory: 024109) and used for optogenetic cortical inhibition in the cortex. D1-eGFP (MMRRC: MMRRC_000297-MU; GENSAT: X60) and D2-eGFP (MMRRC: MMRRC_000230-UNC; GENSAT: S118) were used for slice electrophysiology.

Behavioral Training

Behavioral training was done in standard operant chambers (Med Associates) as described previously (Geddes et al 2018). The operant chamber contained two retractable levers on the left and right side of the front wall, separated by a central food magazine. A house light and a speaker connected to a programmable audio generator were positioned in the back of the chamber. Training protocols were written using MED-PC programming

language and behavioral data was analyzed offline using scripts written in Matlab. Mice were food-restricted for 24 hours prior to training and were maintained at 80-85% of the baseline body weight (before food deprivation). Sucrose pellets were used as rewards in all the behavioral tasks. Mice were first trained with continuous reinforcement (CRF), in which each lever press led to one reward, for a maximum of 10 rewards per session. Mice were trained on this schedule for at least three days and until all 10 rewards were received within 10 minutes. Following CRF, mice were trained with the auditory feedback-assisted action sequence task, a fixed-ratio four schedule. Sessions started with the house light on and extension of both the left and right levers. Following each left lever press, a 100-ms 3kHz pure tone was delivered after a 50ms delay, while following each right lever press, a 100-ms 8kHz pure tone was delivered after a 50ms delay. After every four presses, levers retracted to indicate the end of the trial. Only the four-press sequence composed of left-left-right-right led to the delivery of a reward. The inter-trial interval (ITI) was 5s. Daily sessions ended until 40 reinforcers were acquired, or the session time of three hours was run out. In optogenetic experiments, the reinforcers number was set at 60; in tone deprivation experiments, the number of reinforcers was 20. The efficiency was defined by the percentage of correct sequences (LLRR) in a behavioral session, which was calculated by dividing the number of correct sequences by the total number of four-press sequences. In auditory feedback manipulation experiments, the reinforcers number was set at 60, and 10–30% of trials were randomly selected as the probe trials for tone manipulation. Within one session, manipulation was only done once per sequence for one selected position (for the session) in the probe trials. Sessions were repeated across multiple days to ensure enough trials for analysis.

Stereotaxic surgery

Mice were anesthetized with isoflurane (4% induction; 1%–2% sustained) anesthesia and then placed in a stereotaxic frame (Kopf). For muscimol and DREADDs experiments, 26-gauge guide cannulas (P1 Technologies) were implanted using the following coordinates– Cg/M2: +0.8~1.2 mm AP, ± 0.35 mm ML, –0.5 mm DV; AuD: –2.5 mm AP, ± 4.1 mm ML, –0.8 mm DV; OFC: –2.5 mm AP, ± 1~1.5 mm ML, –1.5 mm DV; the posterior striatum: –1 mm AP, ± 3 mm ML, –2.3 mm DV. Cannulas were cemented in place with Tetric EvoFlow dental cement. Dummy cannulas compatible with the length of the guide cannulas were inserted after surgery. Viral injection was done with a manual syringe (Hamilton) using the following coordinates– Cg/M2: +0.8~1.2 mm AP, ± 0.35 mm ML, -1.2~ –0.8 mm DV; AuD: –2.5 mm AP, ± 4.1 mm ML, –0.9 mm DV; M1: +1.1 mm AP, ± 1.6 mm ML, –0.9 mm DV; OFC: +2.5 mm AP, ± 1~1.5 mm ML, –1.9 mm DV; DMS: +0.5 mm AP, ± 1.4 mm ML, –2.4 mm DV; DLS: 0~+0.3 mm AP, ± 2.5 mm ML, –2.4 mm DV. Optogenetic fiber implants were performed with the following coordinates–Cg/M2: +0.8~1.2 mm AP, ± 0.35~0.4 mm ML, –0.7 mm DV; AuD: –2.5 mm AP, ± 4.1 mm ML, –0.8 mm DV; M1: +1.1 mm AP, ± 1.6 mm ML, -0.9 mm DV; PPC: –2 mm AP, ± 1.5 mm ML, –0.2 mm DV; M2: +1.2 mm AP, ± 0.6 mm ML, -0.15 mm DV; DMS: +0.5 mm AP, ± 1.4 mm ML, -2.3 mm DV; DLS: 0~+0.3 mm AP, ± 2.5 mm ML, -2.3 mm DV; PL:+2 mm AP, ± 0.6 mm ML, -1.3 mm DV with a 15-degree angle.

Muscimol and DREADDs experiments

Following learning, mice were implanted with cannulas and re-trained until they achieved at least 35% behavioral efficiency. The mice then received a three-day infusion protocol as previously described (Geddes et al 2018): day1–vehicle as pre-test control, day2–muscimol (or CNO in DREADDs experiments), and day 3–vehicle as post-test control. CNO (Sigma-Aldrich) was dissolved in a vehicle (saline with DMSO). Muscimol (Sigma-Aldrich) was dissolved in saline. Before infusion, mice were anesthetized with isoflurane, and injection cannulas (projecting 0.2 or 0.5 mm over the guide cannulas) connected to an infusion pump via 28-gauge polyethylene tubing were inserted into the guide cannulas delivery solution. Bilaterally infusion with drugs (vehicle or muscimol/CNO) was done followed by a five-minute waiting time. Mice were placed back in the home cages and started the behavioral task 30 minutes after drug delivery.

Optogenetic experiments

Following learning, mice were implanted with custom-made optrodes consisting of a ceramic ferrule and optic fiber. After recovery for a few days, mice were then re-trained in operant chambers tethered to fiber-optic cables. Optogenetic stimulation sessions began once mice reached 35-40% behavioral efficiency. Optogenetic stimulation was delivered with a 473 nm laser (LaserGlow Technologies), controlled by a programmed TTL output. Within an optogenetic session, stimulation only occurred once per sequence for one selected position (for that session) in randomly selected 10-30% of trials. Stimulation sessions were repeated across multiple days to ensure enough trials for analysis.

In vivo neuronal recording

After learning, mice were implanted with electrode arrays (Innovative Neurophysiology, NC) of 2 x 8 tungsten contacts with each contact 35 um in diameter and spaced 150 um apart in the same row, and 200 μm apart between two rows. After recovery for one week, mice were retrained in operant chambers tethered to a recording cable until reaching 35-40% efficiency. In vivo recording procedures were performed as previously described (Cook et al., 2022). In recording sessions, neural activity was recorded using the MAP system (Plexon). Spike activity was first sorted online with a sorting algorithm and only spikes with typical waveforms and a high signal-to-noise ratio were saved for analysis. The saved spike activities were further offline sorted to identify single units using the sorting software (Plexon). Single units had a clear refractory period in the inter-spike interval histogram, with no spikes during the refractory period. All the timestamps of the behavioral events generated by a Med Associates interface board were sent to and recorded in the MAP recording system. The timestamps for spikes and behavioral events were further analyzed using custom scripts written in Matlab.

Immunohistochemistry

Mice were transcardially perfused with 0.9% saline or 0.01M PBS, followed by 4% paraformaldehyde. Brains were post-fixed in 4% paraformaldehyde overnight at 4 C and transferred to 30% sucrose. Brains were then sectioned with a microtome coronally into 40–55-um uM sections. For staining, free-floating sections were blocked (3% normal horse serum and 0.25% Triton X-100 in TBS) for one hour and incubated with primary antibody overnight

at 4 C. Slices were then washed three times with TBS, incubated with secondary antibody for one hour at room temperature, and washed again before being mounted with mounting media containing DAPI. The following primary antibodies are used: goat anti-cFoS (1:500; sc-52-G), chicken anti-GFP (1:1000; Aves Labs, GFP-1020) and mouse anti-mCherry (1:500; Clontech, 632543). Slices were imaged by confocal microscopy.

Slice electrophysiology

14–20 days following AAV-hSyn-mCherry-ChR2 injection in Cg-M2 of D1 or D2-eGPF mice, we deeply anesthetized them with ketamine/ xylazine mixture and transcardially perfused them with ice cold NMDG cutting solution, saturated with 95% O_2/5% CO_2, containing (in mM): NMDG 105, HCl 105, KCl 2.5, NaH_2PO_4 1.2, $NaHCO_3$ 26, Glucose 25, Sodium L-Ascorbate 5, Sodium Pyruvate 3, Thiourea 2, $MgSO_4$ 10, $CaCl_2$ 0.5 (300mOsm, pH =7.4). We cut 300 µm thick coronal brain slices on a vibratome (Leica VT1000S) through the striatum in ice-cold, bubbling NMDG cutting solution. Slices were recovered for ~15 minutes at 33°C in bubbling NMDG cutting solution followed by 45 min in normal ACSF containing (in mM): NaCl 125, KCl 2.5, NaH_2PO4 1.25, $NaHCO_3$ 25, D-Glucose 12.5, $MgCl_2$ 1, $CaCl_2$ 2 (295 mOsm, pH = 7.4), at 27°C. After at least one hour of recovery, slices were transferred to a recording chamber perfused with ACSF at ~2 mL/min and bubbled with 95% O_2/ 5% CO_2 at 30°C. The regions of interest were confirmed by mCherry expression. Whole cell recordings were performed on neurons expressing eGFP and neighboring eGPF-negative neurons, < 50 µm in distance, under 40X objective lens. 5~7 MΩ Glass pipettes were pulled

on a Sutter P-97 puller. Pipettes were filled with internal solution containing (in mM): CsMeSO3 120, NaCl 5, TEA-Cl 10, HEPES 10, QX-314 (Br- salt) 5, EGTA 1.1, MgATP 4, Na-GTP 0.3 (285 mOsm, pH = 7.3 adjusted with CsOH). After a break, cells were held at -70mV to record AMPA receptor-mediated excitatory currents. Paired pulse light stimulation (473nm, 5~65 mW/mm^2, 2.5ms, 100ms ISI) generated by a 473nm blue DPSS laser system (Laserglow Technologies) were delivered through a 200 μm diameter optic fiber (Thor Labs) positioned close to the patched cell (~50-150μm) at 0.05Hz to induce EPSC. Access or series resistance was ranged from 14-25 MΩ and was monitored online. Any changes greater than 20% were omitted from the analysis. Voltage-clamp recordings were performed using an Axopatch 200B amplifier (Axon Instruments), filtered at 3kHz and digitized at 10kHz. Paired pulse ratio was calculated as the ratio of 2nd to 1st amplitude.

Graphing

Diagrams in the figures were mainly created with BioRender.com.

References

Geddes, C. E., Li, H., & Jin, X. (2018). Optogenetic Editing Reveals the Hierarchical Organization of Learned Action Sequences. *Cell, 174*(1), 32-43 e15. doi:10.1016/j.cell.2018.06.012